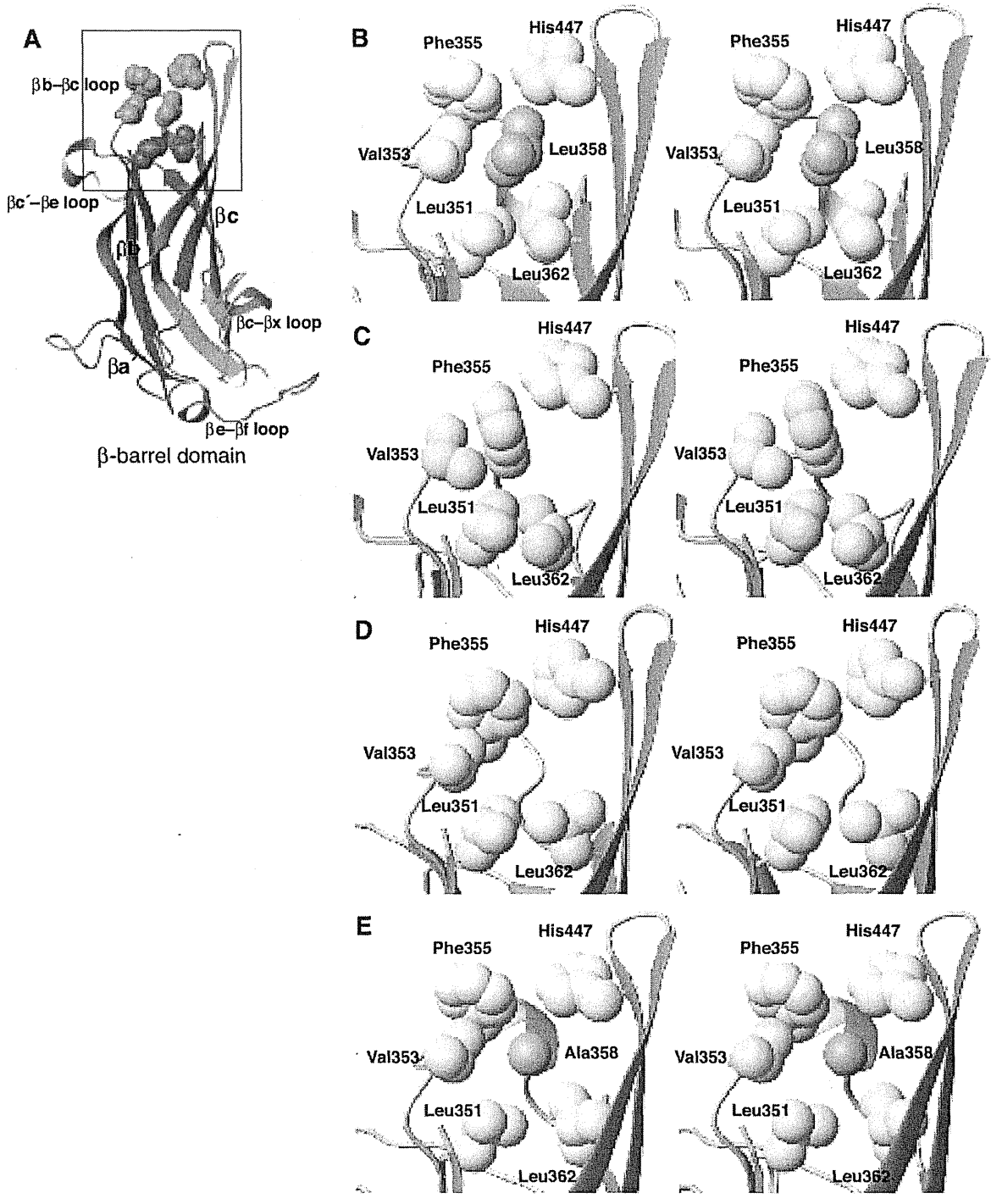

FIG. 9. Structure of the wild-type STAT3 and homology models of the hydrophobic core surrounding Leu358. The crystal structure of the β-barrel domain of the wild-type STAT3β (A) and its hydrophobic core region (B). In panel A, the B-factors are color coded, with lower values in blue and higher values in red, to show that the loop bearing L358 is well-ordered and rigid. (C to E) The hydrophobic core regions of the dD7, dL358, and L358A mutants, respectively. In panels B to E, only the residues corresponding to the boxed region of panel A are shown. The key residue, Leu358, is highlighted in orange, and the surrounding hydrophobic residues that form the core together with Leu358 are shown in yellow. The figures are in stereo view (wall eye) and were produced using MOLMOL (20). It should be noted that all of these modeled core structures are packed less tightly than the wild-type structure.

of the βc strand in the β-barrel domain, as shown in Fig. 5A and 9A. The tertiary structure of this domain appears to be rigid, as its B-factors (ca. 51 Å^2) are considerably lower than those of the other domains of the protein (ca. 66 Å^2). Deletion mutants of the βb strand (dD3 to dD5) resulted in loss of the MgcRacGAP binding ability of STAT3, suggesting that the βb strand is the MgcRacGAP binding site. Interestingly, the MgcRacGAP binding ability and the transcriptional activity of STAT3 were enhanced by deletion of the D6 to D9 region (Fig. 5C). These phenotypes may be explained by the flexibility around the βb strand. Within the β-barrel domain, the DNA-bound βa′-βb loop and the βb-βc loop region are as rigid as the β strands (the B-factors, ca. 40 Å^2), while the βc-βx, βc′-βe, and βe-βf loops are much more flexible (Fig. 9A). The rigidity of the βb-βc loop is probably because Leu358 in this loop is involved in the hydrophobic core formation. When a deletion mutation is introduced in the βb-βc loop (dD6-dD9, d356P, d357E, and d358L), the tertiary structure of the domain may be retained but become more flexible, as the hydrophobic core is packed less tightly than the wild type (see Fig. 9B, C, and D for representative structural models). These STAT3 mutants with more flexibility around the βb strand (binding site of MgcRacGAP) could bind more efficiently to MgcRacGAP, leading to their enhanced activation. In the L358A mutant, which behaves similarly to the d358L mutant (data not shown), the hydrophobic core of the domain is also loosened (Fig. 9E). Thus, all of these deletion and point mutations may destabilize the hydrophobic core of the domain around the βb strand (binding site of MgcRacGAP) and therefore seem to increase the binding ability of the βb strand to MgcRacGAP. The dD2 and dD10 mutants also strongly bind to MgcRacGAP, possibly because of the distortion of the domain structure, while hyperactive transcription was not observed, as they lacked the DNA binding activities. The loss of the MgcRacGAP binding ability in the dD1 mutant lacking the C terminus of the βa′ strand may be due to a secondary result of structural distortion of the βa′ strand and the DNA-bound βa′-βb loop. Our current hypothesis is that upon binding with MgcRacGAP, the β-barrel domain of STAT undergoes some conformational change so that the MgcRacGAP binding region (the βb strand) becomes more flexible and more exposed.

MgcRacGAP accompanied by GTP-bound Rac1 functions both as a mediator of the tyrosine phosphorylation of STATs and as an NLS-containing nuclear chaperone of p-STATs during interphase, while MgcRacGAP plays a critical role in cell division. We believe that MgcRacGAP is a molecule which functions in the nucleocytoplasmic transporting system during interphase and in the mitotic apparatus from metaphase to cytokinesis, as is the case with nucleocytoplasmic transporters, including importins and Ran, which are also involved in the formation of the mitotic spindle after the disassembly of the nuclear envelope (7). Although MgcRacGAP is not involved in nuclear translocation of NF-κB, whether it is involved in nuclear transport of other proteins is still open to question.

ACKNOWLEDGMENTS

We thank Toshio Hirano for kindly providing BaF-BO3 mutants and Dovie Wylie for language assistance.

This work was supported by the RIKEN Structural Genomics/Proteomics Initiative, the National Project on Protein Structural and Functional Analyses, the Sumitomo Foundation, and the Ministry of Education, Culture, Sports, Science and Technology of Japan.

REFERENCES

1. **Adam, S. A., R. S. Marr, and L. Gerace.** 1990. Nuclear protein import in permeabilized mammalian cells requires soluble cytoplasmic factors. J. Cell Biol. **111**:807–816.
2. **Becker, S., B. Groner, and C. W. Müller.** 1998. Three-dimensional structure of the Stat3β homodimer bound to DNA. Nature **394**:145–151.
3. **Bromberg, J. F., M. H. Wrzeszczynska, G. Devgan, Y. Zhao, R.G. Pestell, C. Albanese, and J. E. Darnell, Jr.** 1999. The JAK-STAT pathway: summary of initial studies and recent advances. Stat3 as an oncogene. Cell **98**:295–303.
4. **Chook, Y. M., and G. Blobel.** 2001. Karyopherins and nuclear import. Curr. Opin. Struct. Biol. **11**:703–715.
5. **Darnell, J. E., Jr.** 2002. Transcription factors as targets for cancer therapy. Nat. Rev. Cancer **2**:740–749.
6. **Darnell, J. E., Jr.** 1996. The JAK-STAT pathway: summary of initial studies and recent advances. Recent Prog. Horm. Res. **51**:391–403.
7. **Dasso, M.** 2001. Running on Ran nuclear transport and the mitotic spindle. Cell **104**:321–324.
8. **Fagerlund, R., L. Kinnunen, M. Köhler, I. Julkunen, and K. Melén.** 2005. NF-κB is transported into the nucleus by importin α3 and importin α4. J. Biol. Chem. **280**:15942–15951.
9. **Fiser, A., R. K. Do, and A. Sali.** 2000. Modeling of loops in protein structures. Protein Sci. **9**:1753–1773.
10. **Fukada, T., M. Hibi, Y. Yamanaka, M. Takahashi-Tezuka, Y. Fujitani, T. Yamaguchi, K. Nakajima, and T. Hirano.** 1996. Two signals are necessary for cell proliferation induced by a cytokine receptor gp130: involvement of STAT3 in anti-apoptosis. Immunity **5**:449–460.
11. **Gorlich, D., and U. Kutay.** 1999. Transport between the cell nucleus and the cytoplasm. Annu. Rev. Cell Dev. Biol. **15**:607–660.
12. **Hirose, K., T. Kawashima, I. Iwamoto, T. Nosaka, and T. Kitamura.** 2001. MgcRacGAP is involved in cytokinesis through associating with mitotic spindle and midbody. J. Biol. Chem. **276**:5821–5828.
13. **Ihle, J. N.** 1996. Janus kinases in cytokine signalling. Philos. Trans. R. Soc. Lond. B **351**:159–166.
14. **Isshiki, H., S. Akira, O. Tanabe, T. Nakajima, T. Shimamoto, T. Hirano, and T. Kishimoto.** 1990. Constitutive and interleukin-1 (IL-1)-inducible factors interact with the IL-1-responsive element in the IL-6 gene. Mol. Cell. Biol. **10**:2757–2764.
15. **Jaffe, A. B., and A. Hall.** 2005. Rho GTPases: biochemistry and biology. Annu. Rev. Cell Dev. Biol. **21**:247–269.
16. **Jantsch-Plunger, V., P. Gonczy, A. Romano, H. Schnabel, D. Hamill, R. Schnabel, A.A. Hyman, and M. Glotzer.** 2000. CYK-4: a Rho family gtpase activating protein (GAP) required for central spindle formation and cytokinesis. J. Cell Biol. **149**:1391–1404.
17. **Kawashima, T., Y. C. Bao, Y. Nomura, Y. Moon, Y. Tonozuka, Y. Minoshima, T. Hatori, A. Tsuchiya, M. Kiyono, T. Nosaka, H. Nakajima, D.A. Williams, and T. Kitamura:** 2006. Rac1 and a GTPase activating protein MgcRacGAP are required for nuclear translocation of STAT transcription factors. J. Cell Biol. **175**:937–946.
18. **Kawashima, T., K. Hirose, T. Satoh, A. Kaneko, Y. Ikeda, Y. Kaziro, T. Nosaka, and T. Kitamura.** 2000. MgcRacGAP is involved in the control of growth and differentiation of hematopoietic cells. Blood **96**:2116–2124.
19. **Kinoshita, E., E. Kinoshita-Kikuta, K. Takiyama, and T. Koike.** 2006. Phosphate-binding tag, a new tool to visualize phosphorylated proteins. Mol. Cell. Proteomics **5**:749–757.
20. **Koradi, R., M. Billeter, and K. Wüthrich.** 1996. MOLMOL: a program for display and analysis of macromolecular structures. J. Mol. Graph. **14**:51–55.
21. **Kutay, U., E. I. Izaurralde, F.R. Bischoff, I.W. Mattaj, and D. Görlich.** 1997. Dominant-negative mutants of importin-β block multiple pathways of import and export through the nuclear pore complex. EMBO J. **16**:1153–1163.
22. **Lanning, C. C., R. Ruiz-Velasco, and C. L. Williams.** 2003. Novel mechanism of the co-regulation of nuclear transport of SmgGDS and Rac1. J. Biol. Chem. **278**:12495–12506.
23. **Latimer, M., M. K. Ernst, L. L. Dunn, M. Drutskaya, and N. R. Rice.** 1998. The N-terminal domain of IκBα masks the nuclear localization signal(s) of p50 and c-Rel homodimers. Mol. Cell. Biol. **18**:2640–2649.
24. **Lee, B. J., A. E. Cansizoglu, K. E. Süel, T. H. Louis, Z. Zhang, and Y. M. Chook.** 2006. Rules for nuclear localization sequence recognition by karyopherin beta 2. Cell **126**:543–558.
25. **Liu, L., K. M. McBride, and N. C. Reich.** 2005. STAT3 nuclear import is independent of tyrosine phosphorylation and mediated by importin-alpha3. Proc. Natl. Acad. Sci. USA **102**:8150–8155.
26. **Ma, J., and X. Cao.** 2006. Regulation of Stat3 nuclear import by importin α5 and importin α7 via two different functional sequence elements. Cell Signal. **18**:1117–1126.
27. **Marg, A., Y. Shan, T. Meyer, T. Meissner, M. Brandenburg, and U. Vinkemeier.** 2004. Nucleocytoplasmic shuttling by nucleoporins Nup153 and Nup214 and CRM1-dependent nuclear export control the subcellular distribution of latent Stat1. J. Cell Biol. **165**:823–833.
28. **Marti-Renom, M. A., A. Stuart, A. Fiser, R. Sanchez, F. Melo, and A. Sali.**

2000. Comparative protein structure modeling of genes and genomes. Annu. Rev. Biophys. Biomol. Struct. **29:**291–325.
29. **Mattaj, I., and L. Englmeier.** 1998. Nucleocytoplasmic transport: the soluble phase. Annu. Rev. Biochem. **67:**265–306.
30. **McBride, K. M., G. Banninger, C. McDonald, and N. C. Reich.** 2002. Regulated nuclear import of the STAT1 transcription factor by direct binding of importin-α. EMBO J. **21:**1754–1763.
31. **Michaelson, D., W. Abidi, D. Guardavaccaro, M. Zhou, I. Ahearn, M. Pagano, and M. R. Philips.** 2008. Rac1 accumulates in the nucleus during the G_2 phase of the cell cycle and promotes cell division. J. Cell Biol. **181:**485–496.
32. **Minoshima, Y., T. Hori, M. Okada, H. Kimura, T. Haraguchi, Y. Hiraoka, Y. C. Bao, T. Kawashima, T. Kitamura, and T. Fukagawa.** 2005. The constitutive centromere component CENP-50 is required for recovery from spindle damage. Mol. Cell. Biol. **25:**10315–10328.
33. **Minoshima, Y., T. Kawashima, K. Hirose, Y. Tonozuka, A. Kawajiri, Y.C. Bao, X. Deng, M. Tatsuka, S. Narumiya, W. S. May, Jr., T. Nosaka, K. Semba, T. Inoue, T. Satoh, M. Inagaki, and T. Kitamura.** 2003. Phosphorylation by Aurora B converts MgcRacGAP to a RhoGAP during cytokinesis. Dev. Cell **4:**549–560.
34. **Mishima, M., S. Kaitna, and M. Glotzer.** 2002. Central spindle assembly and cytokinesis require a kinesin-like protein/RhoGAP complex with microtubule bundling activity. Dev. Cell **2:**41–54.
35. **Miura, M., T. Tamura, and K. Mikoshiba.** 1990. Cell-specific expression of the mouse glial fibrillary acidic protein gene: identification of the cis- and trans-acting promoter elements for astrocyte-specific expression. J. Neurochem. **55:**1180–1188.
36. **Morita, S., T. Kojima, and T. Kitamura.** 2000. Plat-E: an efficient and stable system for transient packaging of retroviruses. Gene Ther. **12:**1063–1066.
37. **Onishi, M., T. Nosaka, K. Misawa, A. L. Mui, D. Gorman, M. McMahon, A. Miyajima, and T. Kitamura.** 1998. Identification and characterization of a constitutively active STAT5 mutant that promotes cell proliferation. Mol. Cell. Biol. **18:**3871–3879.
38. **Peifer, M., S. Berg, and A. B. Reynolds.** 1994. A repeating amino acid motif shared by proteins with diverse cellular roles. Cell **76:**789–791.
39. **Ridley, A. J.** 2006. Rho GTPases and actin dynamics in membrane protrusions and vesicle trafficking. Trends Cell Biol. **16:**522–529.
40. **Saharinen, P., K. Takaluoma, and O. Silvennoinen.** 2000. Regulation of the Jak2 tyrosine kinase by its pseudokinase domain. Mol. Cell. Biol. **20:**3387–3395.
41. **Sali, A., and T. L. Blundell.** 1993. Comparative protein modelling by satisfaction of spatial restraints. J. Mol. Biol. **234:**779–815.
42. **Sekimoto, T., N. Imamoto, K. Nakajima, T. Hirano, and Y. Yoneda.** 1997. Extracellular signal-dependent nuclear import of Stat1 is mediated by nuclear pore-targeting complex formation with NPI-1, but not Rch1. EMBO J. **16:**7067–7077.
43. **Tonozuka, Y., Y. Minoshima, Y. C. Bao, Y. Moon, Y. Tsubono, T. Hatori, H. Nakajima, T. Nosaka, T. Kawashima, and T. Kitamura.** 2004. A GTPase activating protein binds STAT3 and is required for IL-6-induced STAT3 activation and for differentiation of a leukemic cell line. Blood **104:**3550–3557.
44. **Ushijima, R., N. Sakaguchi, A. Kano, A. Maruyama, Y. Miyamoto, T. Sekimoto, Y. Yoneda, K. Ogino, and T. Tachibana.** 2005. Extracellular signal-dependent nuclear import of STAT3 is mediated by various importin alphas. Biochem. Biophys. Res. Commun. **330:**880–886.
45. **Van de Putte, T., A. Zwijsen, O. Lonnoy, V. Rybin, M. Cozijnsen, A. Francis, V. Baekelandt, C. A. Kozak, M. Zerial, and D. Huylebroeck.** 2001. Mice with a homozygous gene trap vector insertion in mgcRacGAP die during preimplantation development. Mech. Dev. **102:**33–44.
46. **Wang, J. M., P. Cieplak, and P. A. Kollman.** 2000. How well does a restrained electrostatic potential (RESP) model perform in calculating conformational energies of organic and biological molecules? J. Comput. Chem. **21:**1049–1074.
47. **Wu, X. M., X. L. Tu, K. S. Joeng, M. J. Hilton, D. A. Williams, and F. X. Long.** 2008. Rac1 activation controls nuclear localization of beta-catenin during canonical Wnt signaling. Cell **133:**340–353.
48. **Yamada, T., T. Kurosaki, and M. Hikida.** 2008. Essential roles of MgcRacGAP in multilineage differentiation and survival of murine hematopoietic cells. Biochem. Biophys. Res. Commun. **372:**941–946.
49. **Zeng, R., Y. Aoki, M. Yoshida, K. Arai, and S. Watanabe.** 2002. Stat5B shuttles between cytoplasm and nucleus in a cytokine-dependent and -independent manner. J. Immunol. **168:**4567–4575.

Int J Hematol (2009) 89:470–481
DOI 10.1007/s12185-009-0299-0

ORIGINAL ARTICLE

Possible involvement of RasGRP4 in leukemogenesis

Naoko Watanabe-Okochi · Toshihiko Oki · Yukiko Komeno · Naoko Kato · Koichiro Yuji · Ryoichi Ono · Yuka Harada · Hironori Harada · Yasuhide Hayashi · Hideaki Nakajima · Tetsuya Nosaka · Jiro Kitaura · Toshio Kitamura

Received: 25 January 2009 / Revised: 24 February 2009 / Accepted: 8 March 2009 / Published online: 7 April 2009

Abstract It is now conceivable that leukemogenesis requires two types of mutations, class I and class II mutations. We previously established a mouse bone marrow-derived HF6, an IL-3-dependent cell line, that was immortalized by a class II mutation MLL/SEPT6 and can be fully transformed by class I mutations such as FLT3 mutants. To understand the molecular mechanism of leukemogenesis, particularly progression of myelodysplastic syndrome (MDS) to acute leukemia, we made cDNA libraries from the samples of patients and screened them by expression-cloning to detect class I mutations that render HF6 cells factor-independent. We identified RasGRP4, an activator of Ras, as a candidate for class I mutation from three of six patients (MDS/MPD = 1, MDS-RA = 1, MDS/AML = 2, CMMoL/AML = 1 and AML-M2 = 1). To investigate the potential roles of RasGRP4 in leukemogenesis, we tested its in vivo effect in a mouse bone marrow transplantation (BMT) model. C57BL/6J mice transplanted with RasGRP4-transduced primary bone marrow cells died of T cell leukemia, myeloid leukemia, or myeloid leukemia with T cell leukemia. To further examine if the combination of class I and class II mutations accelerated leukemic transformation, we performed a mouse BMT model in which both AML1 mutant (S291fsX300) and RasGRP4 were transduced into bone marrow cells. The double transduction led to early onset of T cell leukemia but not of AML in the transplanted mice when compared to transduction of RasGRP4 alone. Thus, we have identified RasGRP4 as a gene potentially involved in leukemogenesis and suggest that RasGRP4 cooperates with AML1 mutations in T cell leukemogenesis as a class I mutation.

Keywords RasGRP4 · AML1 · Class I mutation · Leukemogenesis · cDNA library

Electronic supplementary material The online version of this article (doi:10.1007/s12185-009-0299-0) contains supplementary material, which is available to authorized users.

N. Watanabe-Okochi · T. Oki · Y. Komeno · N. Kato · H. Nakajima · J. Kitaura · T. Kitamura (✉)
Division of Cellular Therapy, Advanced Clinical Research Center, The Institute of Medical Science, The University of Tokyo, 4-6-1 Shirokanedai, Minato-ku, Tokyo 108-8639, Japan
e-mail: kitamura@ims.u-tokyo.ac.jp

K. Yuji
Division of Molecular Therapy, Advanced Clinical Research Center, The Institute of Medical Science, The University of Tokyo, Tokyo, Japan

R. Ono · T. Nosaka
Department of Microbiology, Mie University Graduate School of Medicine, Tsu-shi, Japan

Y. Harada
International Radiation Information Center, Research Institute for Radiation Biology and Medicine, Hiroshima University, Hiroshima, Japan

H. Harada
Department of Hematology and Oncology, Research Institute for Radiation Biology and Medicine, Hiroshima University, Hiroshima, Japan

Y. Hayashi
Department of Hematology/Oncology, Gunma Children's Medical Center, Shibukawa, Japan

1 Introduction

Various chromosome translocations and gene mutations were known to participate in leukemogenesis. Recently, it was recognized that multiple gene alterations are required

for leukemogenesis; coexistence of chromosomal translocations and gene mutations are frequently found in the same patient. There are some frequent combinations including c-Kit mutations and AML1/ETO [1–6], c-Kit mutations and inv(16) [1, 5–7], Ras mutations and AML1 point mutations [8, 9], FLT3-ITD and AML1 point mutations [10, 11], FLT3 mutations and PML-RARα [12–16], MLL rearrangement and FLT3-TKD [17], MLL rearrangement and Ras mutations [18], and FLT3-ITD and NPM1 mutations [19]. Interestingly, on the other hand, RAS and FLT3 mutations, which are detected in about 50% of patients with de novo AML, are negatively associated with each other [20, 21]. In mice models, while expression of PML/RARα in transgenic mice caused a nonfatal myeloproliferative syndrome, transplantation of bone marrow cells obtained from PML/RARα transgenic mice retrovirally transduced with FLT3-ITD resulted in development of an APL-like disease in a short latency [22]. Two step leukemogenesis was also suggested by an in vitro culture system of human hematopoietic cells [23]. Based on these findings, leukemia-related mutations are classified into two groups, class I and class II mutations. Class I mutations include activating mutations of tyrosine kinases and a small GTPase Ras or inactivation of apoptosis-related molecule, and these mutations induce cell proliferation or block apoptosis. On the other hand, class II mutations include dominant negative mutations of transcription factors involved in differentiation of hematopoietic cells, such as AML1/ETO, PML/RARa, or constitutively activated mutations of chromosome remodeling factors such as MLL-related fusion genes [24]. Indeed, it has been reported that a combination of class I and II mutations such as PML/RARα plus FLT3-ITD [22], AML1/ETO plus FLT3 mutation [25], AML1/EVI1 plus BCR/ABL [26], MLL/SEPT6 plus FLT3 mutation [27], K-ras plus PML/RARα [28] induced AML in a mouse BMT model, while either class I or II mutation alone led to, myeloproliferative disorders (MPD) or MDS like disease, not leukemia [22–28].

To identify class I mutations from patients with MDS/AML, MPD, or AML, we used retrovirus-mediated expression cloning; cDNA libraries from patients' samples were constructed and retrovirally transfected into an IL-3-dependent myeloid cell line, HF6, immortalized by a class II mutation MLL/SEPT6 [27]. We searched for class I mutations that abrogate IL-3 dependency of HF6 and we identified RasGRP4 as a candidate gene from three different libraries (MDS/MPD = 1, MDS/AML = 1, MDS-RA = 1). In addition, FLT3-ITD was identified in a patient with MDS/AML.

RasGRP4 belongs to a family of guanine nucleotide-exchange factors (RasGRP1-4) that positively regulate Ras and related small GTPases, and is mainly expressed in myeloid cells and mast cells [29, 30]. RasGRP4 appears to act downstream of the tyrosine kinase receptor c-Kit/CD117 [30]. RasGRP4 is located on 19q13.1 and alterations of this site have been found in several cancers (the "Cancer Chromosomes" at the NCI web site), and was previously isolated by expression cloning from cytogenetically normal AML patients using the focus-forming assay of NIH3T3 cells [29]. In the present study, we isolated RasGRP4 using expression cloning as a gene that fully transforms IL-3-dependent HF6 cells, and investigated the effect of RasGRP4 overexpression in a mouse BMT model and implicated RasGRP4 in leukemogenesis.

2 Materials and methods

2.1 Cell lines and cell culture

A mouse pro-B line Ba/F3 was maintained in RPMI1640/10% fetal bovine serum (FBS) containing 1 ng/ml recombinant mouse IL-3 (obtained from R & D systems). HF6, which had been established by introducing MLL/SEPT6 into mouse bone marrow cells, was maintained in RPMI1640/10% FBS containing 10 ng/ml mouse IL-3 as described [27].

2.2 Screening of cDNA libraries

Complementary cDNA libraries were generated from patients leukemic or MDS cells (MDS/MPD = 1, MDS/AML = 2, CMMoL/AML = 1, MDS-RA = 1, AML-M2 = 1) as described [31]. MDS or leukemic cells of these patients did not harbor recurrent chromosomal translocations involving AML1 or MLL. One patient with AML-M2 did not display t(8;21). The point mutations of AML1 were not screened. Recombinant retroviruses were generated by transient transfection using an ecotropic packaging cell line PLAT-E as described with minor modifications [32]. Bone marrow or peripheral blood samples of patients were taken under the experimental procedure approved by the ethical committees of our institute (approve no. 20-9).

We introduced each cDNA library into two IL-3-dependent cell lines Ba/F3 and HF6. After transduction with the cDNA library, the transduced cells were seeded into 96-well plates in the absence of IL-3, and factor independent clones were isolated. To identify the cDNA that confers factor independency on Ba/F3 or HF6, genomic DNA of the factor independent clones were purified and integrated cDNAs were isolated and sequenced.

2.3 Vector construction

cDNAs for human RasGRP4 were cloned from cDNA libraries of MDS/MPD patients and normal volunteers using PCR primers: 5′-GGAGCTGAGCCCTACTCTTG-3′

(forward), 5′-AGAGTCTGACGGCAGGACTC-3′ (reverse). We used pfu polymerase (Stratagene, La Jolla, CA) to amplify the coding region of human RasGRP4. We subcloned the PCR products into TOPO vector (Invitrogen, San Diego, CA). Then, the EcoRI fragment carrying RasGRP4 was inserted into the EcoRI sites of pMXs vector [32]. RasGRP4 sequences derived from patients and normal volunteers were not identical to those in the data bases as described in result section. We used an AML1 mutant, S291fsX300, identified from case number 27 among MDS/AML patients [33]. This mutant is hereafter referred to as AML1-S291fs. The AML1-S291fs was inserted upstream of the IRES-EGFP cassette of a retrovirus vector pMYs-IG [32] to generate pMYs-AML1-S291fs-IG.

2.4 Expression of RasGRP4 in HF6

To confirm that the isolated RasGRP4 is responsible for factor-independency of HF6, the cells were infected with the retroviruses harboring pMXs-RasGRP4 derived from patients, normal volunteers or an empty vector as a control, and cultured in the absence of IL-3. To investigate the activation of the Ras pathway in the HF6 cells expressing RasGRP4, the transfected cells were lysed in lysis buffer, and lysates were subject to western blot analysis as described with minor modifications [34]. Monoclonal mouse anti-phospho-p44/42 MAPK (Thr^{202}/Tyr^{204}) antibody (Sigma) was used for phosphorylated ERK1/2.

2.5 Bone marrow transplantation

Bone marrow mononuclear cells were isolated and cultured as described [35]. The prestimulated cells were infected for 60 h with the retroviruses harboring pMXs-RasGRP4 derived from a patient with MDS/MPD, pMYs-AML1-S291fs-IG or an empty vector as a control, using six well dishes coated with RetroNectin (Takara Bio, Inc.) according to the manufacturer's recommendations. Then, $0.3–1.2 \times 10^6$ of infected bone marrow cells (Ly-5.1) were injected through tail vein into C57BL/6 (Ly-5.2) recipient mice (8–12 weeks of age) which had been administered a sublethal dose of 5.25 Gy total-body γ-irradiation (135Cs). Overall survival of the transplanted mice was analyzed using the Kaplan–Meier-method. All animal studies were approved by the Animal Care Committee of the Institute of Medical Science, The University of Tokyo.

2.6 Analysis of the transplanted mice

Engraftment of bone marrow cells was confirmed by measuring the percentage of Ly-5.1-positive and/or GFP positive cells in peripheral blood obtained every 1–2 months after the transplant. After the morbid mice were euthanized, their tissue samples including peripheral blood (PB), bone marrow (BM), spleen, liver, and kidney were analyzed. Circulating blood cells were counted by automatic blood cell counter KX-21 (Sysmex, Kobe, Japan). Morphology of the peripheral blood cells was evaluated by staining of air-dried smears with Hemacolor (Merck). Tissues were fixed in 10% buffered formalin, embedded in paraffin, sectioned, and stained with hematoxylin and eosin (H & E). Cytospin preparations of bone marrow and spleen cells were also stained with Hemacolor. The percentage of blasts, myelocytes, neutrophils, monocytes, lymphocytes, and erythroblasts was estimated by examination of at least 200 cells. To assess whether the leukemic cells were transplantable, $2 \times 10^5–1 \times 10^6$ total BM cells including blasts were injected into the tail veins of sublethally irradiated mice. A total of two or three recipient mice were used for each serial transplantation.

2.7 Flow cytometric analysis

Peripheral blood or single-cell suspensions of bone marrow and spleen were stained with the following phycoerythrin (PE)-conjugated monoclonal antibodies: Ly-5.1, Gr-1, CD11b, B220, CD3, CD4, CD8, CD41, c-Kit, Sca-1, CD34, and Ter-119. Then, flow cytometric analysis was performed as described [35].

2.8 RT-PCR

To confirm expression of human RasGRP4, total RNA was extracted from BM cells of transplanted mice using Trizol (Invitrogen, California, USA) and cDNA was prepared with the Superscript II RT kit (Invitrogen, California, USA) and RT-PCR was performed using a 2720 Thermal cycler (Applied Biosystems, Tokyo, Japan). The cDNA was amplified using AmpliTaq Gold (Applied Biosystems by Roche Molecular Systems, Inc., New Jersey. USA). The reaction was subject to one cycle at 95°C for 5 min, 30 cycles of PCR at 95°C for 30 s, 55°C for 30 s, and 72°C for 30 s. All samples were independently analyzed at least three times. The following primer pairs were used: 5′-ACTGGCTGATGCGACACCC-3′ (forward) and 5′-GAGATGGCACTGTGACACAG-3′ (reverse) for human RasGRP4, 5′-ACCACAGTCCATGCCATCAC-3′ (forward) and 5′-TCCACCACCCTGTTGCTGTA -3′ (reverse) for GAPDH.

2.9 Quantitative RT-PCR

To examine expression levels of human RasGRP4 in patients, quantitative RT-PCR was performed. Quantitative RT-PCR was performed using a LightCycler Workflow System (Roche Diagnostics, Mannheim, Germany).

Complementary DNAs derived from bone marrow cells of leukemia or MDS patients as well as normal bone marrow cells were amplified using a SYBR Premix EX Taq (TAKARA). The reaction was subject to one cycle at 95°C for 30 s, 45 cycles of PCR at 95°C for 5 s, 55°C for 10 s, and 72°C for 10 s. All samples were independently analyzed at least three times. The primer pairs for human RasGRP4 and GAPDH were the same as described above. The samples from the patients were obtained under written consents which had been approved by the local ethical committee of each institute or hospital.

2.10 Bubble PCR

Genomic DNA was extracted from BM or spleen cells of transplanted mice and digested with EcoRI, and then the fragments were used for Bubble PCR to identify the integration sites of the retroviruses as described [35]. We confirmed inverse repeat sequence "GGGGGTCTTTCA" as a marker of junction between genomic DNA and retrovirus sequence.

3 Results

3.1 RasGRP4 induces factor-independent growth of HF6

In the screening of cDNA libraries, some wells gave rise to cell growth in the absence of IL-3 from HF6 but not from BaF3 cells. The factor-independent clones were isolated and the cDNAs integrated in the genome DNA were sequenced using PCR. FLT3-ITD was identified in one MDS/AML patient. In addition, RasGRP4 was identified from three different libraries (MDS/MPD = 1, MDS/AML = 1, and MDS-RA = 1). We introduced the isolated RasGRP4 into HF6 to confirm that RasGRP4 was responsible for autonomous growth of HF6 cells (Fig. 1a). In the sequence of RasGRP4 derived from the MDS/MPD, MDS/AML and MDS-RA patients, we found several different amino acids that compared with the sequences in two databases GenBank (accession number AF448437) and GenBank (accession number AY048119) (Table 1). Therefore, we introduced RasGRP4 derived from a patient and two Japanese normal volunteers (normal 1 and 2 in Table 1) into HF6 cells to examine if RasGRP4 from normal volunteers also gives rise to factor-independency. As a result, RasGRP4 from normal volunteers also induced factor-independent growth of HF6, indicating that overexpression of RasGRP4 by itself induced transformation of the cells, independent of some mutations in the amino acid sequence of RasGRP4. While several gene alterations were observed in the samples of patients, we focused on E468K because this change was observed only in a patient with MDS/MPD but not in the sequence derived from the two databases and two normal volunteers (Table 1). However, we did not find any functional importance of the alteration at codon 468 that changes a glutamic acid to a lysine. Moreover, SNPs of this gene are not correlated with lymphoma and leukemia (Y. Nakamura, unpublished results).

To assess the RasGRP4-mediated Ras activation, we examined phosphorylation of ERK1/2 using HF6-cells-transduced RasGRP4. Stimulation with IL-3 induced much stronger phosphorylation of ERK1/2 in the HF6 cells expressing RasGRP4 when compared with parent HF6 cells (Fig. 1b, lanes 6–8). Although we did not observe enhanced phosphorylation of ERK1/2 in the cells overexpressing RasGRP4 without IL-3 (Fig. 1b, lane 5), we assume that non-detectable enhancement of ERK1/2 was

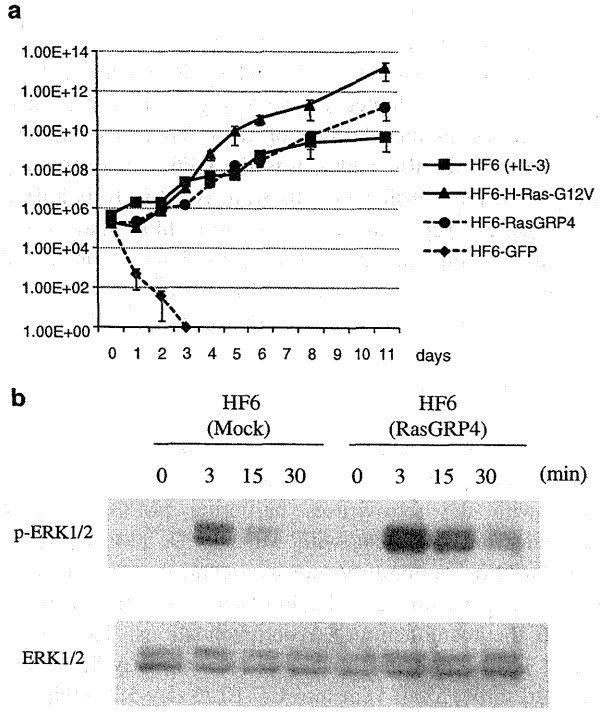

Fig. 1 RasGRP4 conferred factor independency on HF6. **a** HF6 cells expressing the H-Ras-G12V, RasGRP4 and GFP vector were deprived of IL-3, and cells were counted by trypan blue exclusion. The parental HF6 cells in the presence of IL-3 (10 ng/mL) were counted as same. **b** Stimulation with IL-3 induced strong phosphorylation of ERK1/2 in the HF6 cells expressing RasGRP4. Phosphorylation of ERK1/2 (pERK1/2) was examined in HF6 cells transfected with RasGRP4 or empty by western blot analysis using anti-phospho-p44/42 MAPK (Thr^{202}/Tyr^{204}) Ab. Loading amount was estimated by re-probing immunoblots with Abs specific for ERK1/2. The transfected HF6 cells were washed with PBS twice and cultured in RPMI1640/10% FBS without IL-3 for 4 h. Then, some of cells were collected and lysed (*lanes 1 and 5*). The remained cells were stimulated with IL-3 (100 ng/mL) for the indicated period and collected and lysed (*lanes 2–4*, and *6–8*)

Table 1 Polymorphism of RasGRP4

Position of amino acid	AF448437	AY048119	Patient 1 (MDS/MPD)	Patient 2 (MDS/AML)	Patient 3 (MDS-RA)	Normal 1	Normal 2
18	T	T	T	I	T	T	I
120	Q	L	Q	Q	Q	Q	Q
261	R	C	R	R	R	R	R
468	E	E	K	E	E	E	E
541	H	H	H	H	H	H	Y
671	L	P	P	L	L	L	L

enough to induce factor-independent growth of HF6. Only weak activation of the signaling molecule, even non-detectable in biochemical experiments, sometimes induces autonomous cell growth.

3.2 RasGRP4 induced myeloid leukemia and T cell leukemia in mice

We further examined if overexpression of RasGRP4 induced leukemia in a mouse BMT model. We confirmed expression of human RasGRP4 in BM cells of transplanted mice by RT-PCR (Fig. 2a). Transduction of RasGRP4 (E468K) induced myeloid and/or T cell leukemia with various phenotypes, and the transplanted mice died within 2–8 months after the transplantation (Fig. 2b). For example, a mouse (ID 402) died of T cell leukemia with thymoma (weight of thymus was 1,416 mg) and hepatosplenomegaly on day 252 after the transplantation. Leukemic cells showed a CD4- and CD8-double-positive phenotype (Fig. 3). One other mouse developed a similar disease (ID 401). Unfortunately, this mouse died on day 224 before we found out. Therefore, we could only confirm hepatosplenomegaly and a giant thymoma after the death. Two mice (ID 407 and 408) died of AML with hepatosplenomegaly on days 47 and 66 after the transplantation. Severe leukocytosis, anemia and thrombocytopenia were observed in a mouse (ID 408), but severe pancytopenia was observed in the other mouse (ID 407). Leukemic cells of the mouse (ID 408) in bone marrow and thymus uniformly expressed Gr1, CD11b, and B220 on their surfaces (Fig. 3). Four of the transplanted mice (ID 403, 404, 405 and 406) developed both myeloid and T cell leukemia with hepatosplenomegaly, and in some cases, thymoma (ID 404, 405 and 406). In the mouse ID 404, both myeloid and T cell leukemia cells were observed in the bone marrow, while peripheral blood was occupied with myeloid leukemia and thymus was occupied with T cell leukemia (Figs. 3, 4). In summary, two mice died of AML after a short latency (days 47 and 66), two mice died of T cell leukemia after a long latency (days 224 and 252), and four mice died of AML and T cell leukemia (days 76, 83, 129, and 248). The

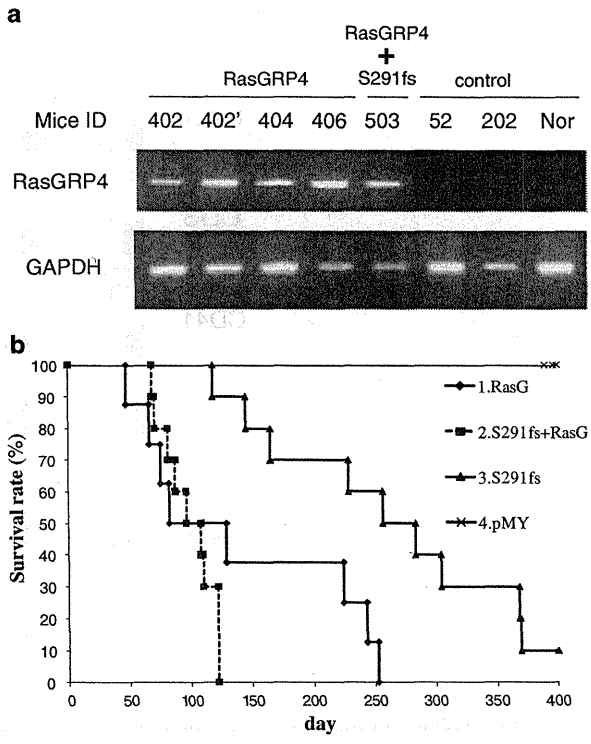

Fig. 2 Co-transduction of RasGRP4 and AML1-S291fs led to early onset of leukemia. **a** Expression of retrovirally introduced RasGRP4 in BM cells. Total RNA from BM cells of transplanted mice were extracted, and the derived cDNAs were subjected to RT-PCR. Mice IDs were shown on the top of the panel. ID 402′ is a second recipient of ID 402. Controls are AML1-S291fs (ID 52), empty vector (ID 202), and normal mouse (Nor). **b** Kaplan–Meier analysis for the survival of mice transplanted with RasGRP4, AML1-S291fs, and double-transduced BM cells. Average survival of RasGRP4 alone (139.8 days) was not significantly different when compared with double transduced mice (101.5 days) ($P = 0.223$, log rank test). Average survival of the double transduced mice (101.5 days) was significantly shorter than that of AML1-S291fs-transduced mice (263.6 days) ($P = 0.00003$, log rank test). RasGRP4 ($n = 8$), AML1-S291fs ($n = 10$), RasGRP4 + AML1-S291fs ($n = 11$), mock ($n = 16$) transduced bone marrow cells were transplanted to mice

details of individual mice are shown in Table 2 and Fig. 5. To assess whether the leukemic cells were transplantable, 2×10^5–1×10^6 total BM cells including blasts were

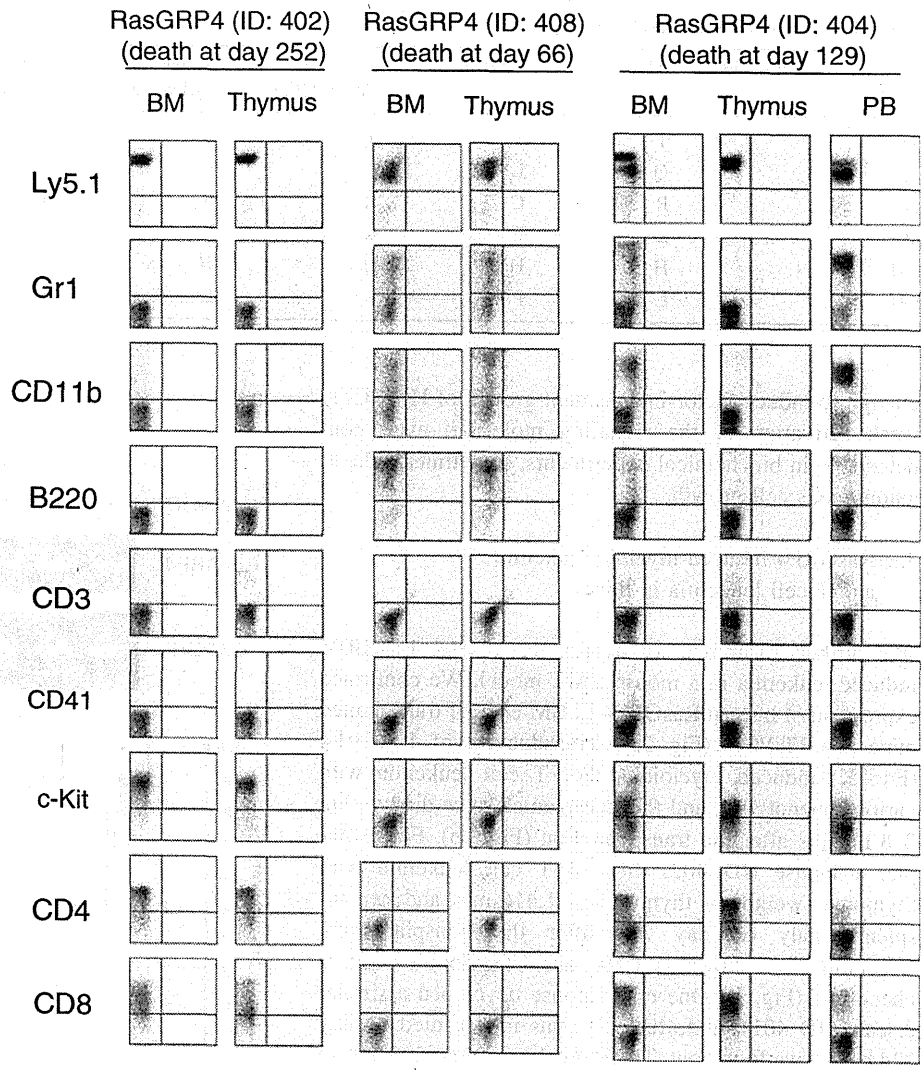

Fig. 3 RasGRP4 induced T cell leukemia and myeloid leukemia in the BMT model. The *dot plots* show Ly5.1, Gr-1, CD11b, B220, CD3, CD41, c-kit, CD4, or CD8 expression detected by corresponding PE-conjugated mAb

injected into recipient mice. We confirmed that both T cell leukemia and myeloid leukemia cells were serially transplantable although the phenotypes slightly changed after the serial transplantation (Supplemental Fig. 1).

3.3 Different integration sites were identified from T cell or myeloid leukemia cells derived from an individual mouse

To examine if the T cell and myeloid leukemia cells were derived from different clones or the same clone, we identified the integration sites in genomic DNA samples of thymus, peripheral blood or bone marrow cells. As shown in Table 3, different integration sites were identified from T cell and myeloid leukemia cells derived from an individual mouse, suggesting that T cell and myeloid leukemic cells were derived from different clones.

The integration near the Samsn1 gene was found twice in ID 405 and ID 406. These mice were transplanted on the same day. The integration site was identical among these leukemic cells indicating that leukemic cells of the two cases were derived from a single hematopoietic progenitor. This result suggests that the integration induced expansion of the transduced stem cells during the 3-day-culture period before the transplantation. Indeed, the mice with the integration at Samsn1 site developed AML with the same phenotype (CD11b positive) and similar latencies (83 and 76 days). On the other hand, different T lineage clones grew up in thymus and developed thymoma.

3.4 RasGRP4 cooperates with an AML1 mutant in leukemogenesis

RasGRP4 appears to function downstream of the tyrosine kinase receptor c-Kit/CD117 [30]. High expression of c-kit

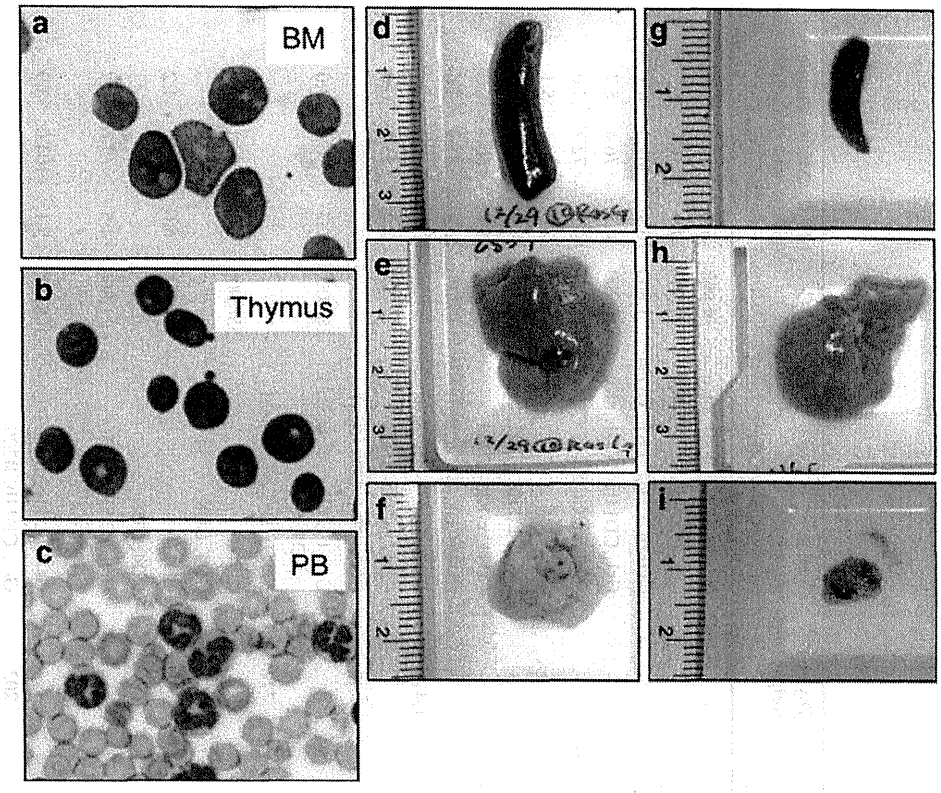

Fig. 4 RasGRP4 induced both of T cell leukemia and myeloid leukemia in the same mouse. Giemsa-stained cells derived from **a** bone marrow, **b** thymus, and **c** peripheral blood obtained from mouse ID 404. Macroscopic findings of **d** spleen, **e** liver, **f** thymus from mice ID 404; *left* **g** spleen, **h** liver, **i** thymus from normal mice; *right* are shown. Images (**a**, **b**, **c**) were obtained with a BH51 microscope and DP12 camera (Olympus, Tokyo, Japan); objective lens, UPlanFl (Olympus); ×1,000

has been found in 60–80% of AML [36] and higher expression is observed in 81.3% of patients with t(8;21) when compared with the patients with other leukemias [2]. Niimi et al. [9] reported that MDS/AML arising from AML1/RUNX1 mutations frequently involves receptor tyrosine kinase (RTK)-RAS signaling pathway activation. We have recently demonstrated that bone marrow cells transduced with AML1 mutants induced MDS-like symptoms after a long latency [35]. Therefore, we also tested if the combination of RasGRP4 and AML1-S291fs, one of the AML1 mutants, induced rapid leukemic transformation in a BMT model. As a result, co-transduction of RasGRP4 and AML1-S291fs led to early death in the transplanted mice (average 101.5 days, $n = 11$) than the expression of RasGRP4 alone (average 139.8 days, $n = 8$) (Fig. 2b). We diagnosed the double-transfected disease mice as T cell leukemia because of enlarged thymus, hepatosplenomegaly, and expansion of blast expressing CD3, CD4, and CD8 in bone marrow, peripheral blood, and thymus (Fig. 6). The onset of T cell leukemia was significantly earlier in the RasGRP4 + AML1 mutant (average 102.7 days, $n = 9$) than RasGRP4 alone (average 238 days, $n = 2$). On the other hand, onset of AML was not significantly changed between RasGRP4 + AML1 mutant (average 96 days, $n = 2$) and RasGRP4 alone (average 56.5 days, $n = 2$) transplanted mice.

3.5 RasGRP4 was overexpressed in some patients with hematological malignancies

We examined expression levels of RasGRP4 in patients with myeloid or T lineage hematological malignancies. As shown in Fig. 7, cells from some patients (T-ALL, AML-M1, MDS-RAEB, MDS-RA, CMMoL) overexpressed RasGRP4.

4 Discussions

We identified RasGRP4 from patients' cDNA libraries as a gene that renders IL-3-dependent HF6 cells factor independent when expressed at high levels via retrovirus-mediated gene transfer. Although we did not find any gain-of-function mutation of RasGRP4 in three patients from whom we identified cDNA for RasGRP4, and we detected high expression of RasGARP4 in only one out of the three patients, it is possible that overexpression or activating mutations are found in patients with malignant diseases including leukemia and MDS. Thus, RasGRP4 is a candidate gene for class I mutations. In addition to RasGRP4, we also identified FLT3-ITD from a patient with MDS/AML, thus showing the feasibility of our functional cloning strategy. The HF6 cells were immortalized by expression

Table 2 Hematological data of the transplanted mice

Gene	Mice ID	GFP (%)	Ly5.1 of BM (%)	Ly5.1 of Thymus (%)	Period from BMT (day)	Spleen weight (mg)	Liver weight (mg)	Thymus weight (mg)	Suefice markers of GFP positive cells	WBC (μL)	Hb (g/dL)	MCV (fL)	Platelet (×1,000/μL)
S291fs	51	27.4	39.8	–	368	153	1,236	–	Gr1, CD11b, CD41, cKit	4,800	6.6	60.0	27.0
S291fs	52	47.8	83.0	–	256	90	1,568	–	Gr1, CD11b, CD41, cKit	4,500	9.9	59.8	38.3
S291fs	54	29.8	45.3	–	304	338	1,812	–	CD11b, CD41, cKit, CD34	1,800	10.4	61.3	4.1
S291fs	55	75.2	83.1	–	165	166	1,574	–	Gr1, CD11b, CD41, cKit,	1,200	4.8	76.4	5.7
S291fs	56	54.9	85.2	–	118	73	1,318	–	CD41, cKit, Sca1, CD34,	2,900	4.5	72.7	4.6
S291fs	57	–	–	–	145	181	1,249	–	–	5,700	2.4		5.1
S291fs	58	72.7	56.5	–	228	225	1,582	–	Gr1, CD11b, CD41, cKit	2,100	9.9	62.7	26.7
S291fs	60	76.3		–	369	186	1,682	–	CD41, c-Kit, CD34	7,500	11.1	66.1	22.2
RasGRP4	402	–	96.5		252	318	1,975		CD4, CD8, c-Kit, Sca1	20,700	12.3	51.9	3.6
				98.9				1,416	CD4, CD8, c-Kit, Sca1				
RasGRP4	403	–	93.5		248	696	2,138		CD41, c-Kit, CD34	8,400	7.2	55.1	0.0
				85.9				92	CD3, CD4, CD8, Sca1				
RasGRP4	404	–	93.9		129	714	2,557		Gr1, CD11b, c-Kit, Sca1, CD4, CD8	282,000	11.7	56.6	3.0
				99.7				777	CD4, CD8, c-Kit, Sca1				
RasGRP4	405	–	91.3		83	1,184	3,699		CD11b	558,900	7.2	57.1	9.9
				98.3				139	CD4, CD8				
RasGRP4	406	–	94.8		76	1,348	2,678		CD11b	96,900	6.6	59.7	1.2
				99.5				609	CD4, CD8				
RasGRP4	407	–	32.0		47	670	4,795		Gr1, CD11b, c-Kit	1,800	4.5	67.6	2.7
				17.1				95	CD3, CD4, CD8				
RasGRP4	408	–	95.7		66	1,110	4,155		Gr1, CD11b, B220	108,900	5.1	104.0	3.9
				93.5				202	Gr1, CD11b, B220				
S291fs + RasGRP4	503	92.1	92.1		96	1,180	6,065		CD3, CD4, CD8	33,600	10.3	64.5	9.3
		95.0		95.0				112	CD3, CD4, CD8				
S291fs + RasGRP4	507	–	–		68	302	–		CD3, CD4, CD8				
				–				805	CD3, CD4, CD8				
S291fs + RasGRP4	513	75.8	80.7		130	544	2,784		CD3, CD8	59,500	10.7	68.8	2.2
		83.8		90.9				155	CD3, CD8				

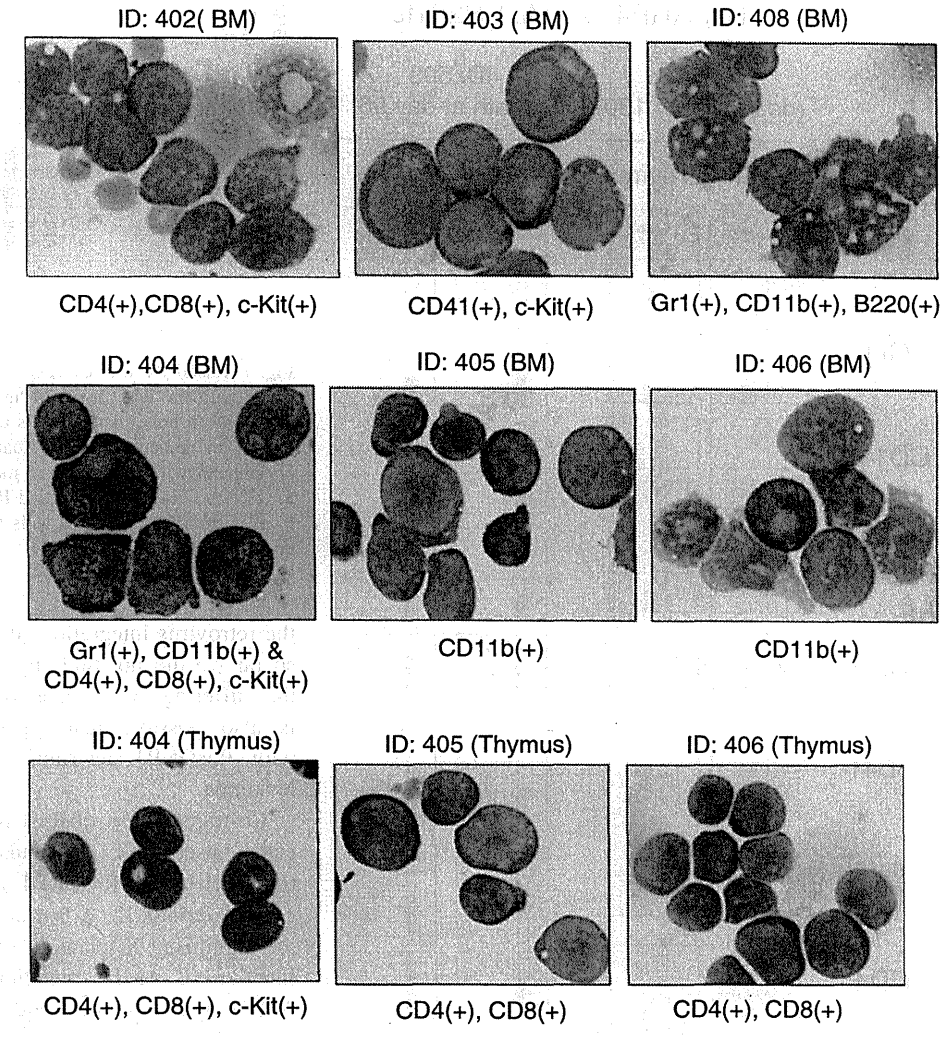

Fig. 5 Morphology of leukemic cells induced by RasGRP4. Giemsa staining photos of the leukemic cells are shown. Mice IDs were shown at *top of the panel*. Surface expression proteins were shown at bottom of the panel. Images were obtained with a BH51 microscope and DP12 camera (Olympus, Tokyo, Japan); objective lens, UPlanFl (Olympus); magnification, ×1,000

Table 3 Retroviral integration sites in the transplanted mice

Mice ID	Sample	Chr. number	Nearest gene	Gene ID	Distance to gene (start or end)	Location	Forward or reverse orientation	RTCGD hits
404	Thymus	10	Bcr	110279	Disrupt CDS	Intron 8	F	0
404	PB	15	Trio	223435	Disrupt CDS	Intron 9	F	3
405	Thymus	14	LOC100042147	100042147	12,962 bp	3′	R	0
405	BM	16	Samsn1	67742	95,998 bp	5′	R	2
406	Thymus	18	LOC100042131	100042131	Disrupt CDS	Exon 2	F	0
406	BM	16	Samsn1	67742	95,998 bp	5′	R	2

of MLL-SEPT6, and can be transformed by oncogenic Ras and Ras-related signals (manuscript in preparation). Therefore, HF6 is a suitable cell line for identification of Ras mutations as well as mutations of Ras-related signaling molecules. On the other hand, Ba/F3 cells can be transformed by STAT5 activation. In addition to these two cell lines, we have developed several other IL-3-dependent bone marrow-derived cell lines immortalized by class II mutations or related molecules (unpublished results). Because these IL-3-dependent cell lines have different signaling profiles, they would be applicable for identification of mutations in a variety of signaling molecules, providing a versatile system for functional cloning of oncogenic mutations.

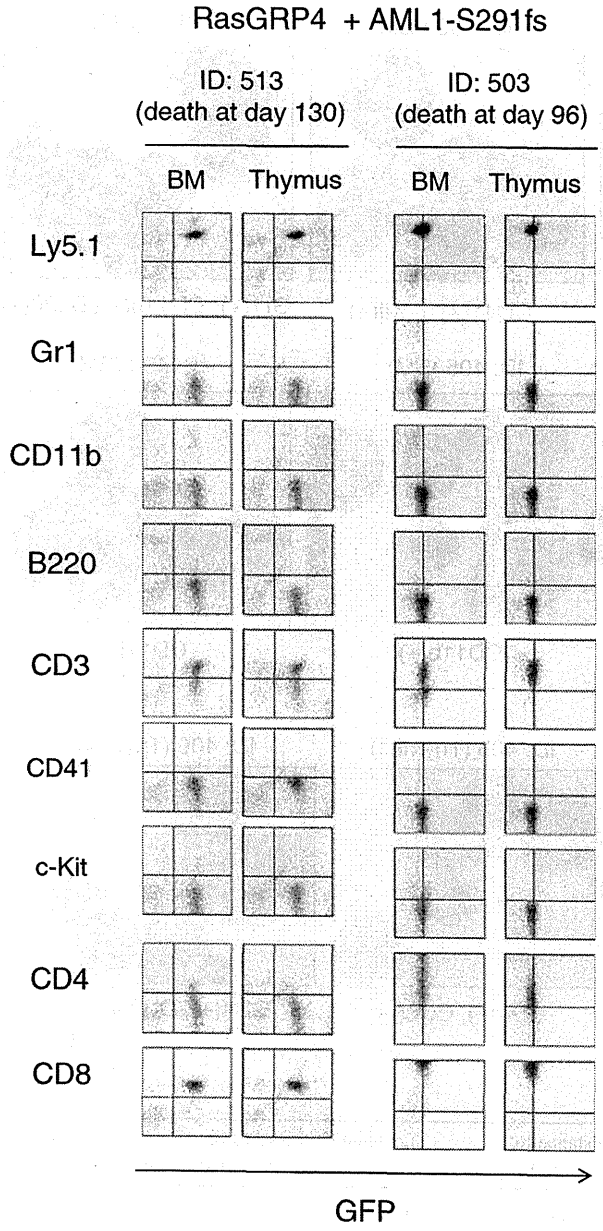

Fig. 6 RasGRP4 and AML1-S291fs induced T cell leukemia in the BMT model. The *dot plots* show Ly5.1, Gr-1, CD11b, B220, CD3, CD41, c-kit, CD4, or CD8 expression detected by corresponding PE-conjugated mAb

Overexpression of RasGRP4-induced T cell leukemia and/or myeloid leukemia in a mouse BMT model. We found that four of eight mice developed both types of leukemia and two mice died of AML after a short latency, while others died of T cell leukemia after a long latency when transplanted with RasGRP4 alone. At present, it is not clear what determines the different phenotypes of leukemia induced by RasGRP4. Although

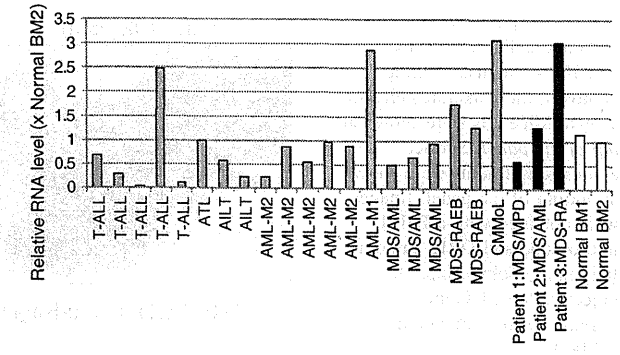

Fig. 7 RasGRP4 was overexpressed in a patient with T-ALL and some patients with myeloid malignancies. Expression levels of RasGRP4 in bone marrow cells derived from patients with hematological malignancies were evaluated by quantitative RT-PCR. *Gray bar* patients with hematological malignancies, *black bar* patients used for cDNA library and identified RasGRP4, *white bar* normal. RNAs from normal bone marrow cells served as a control (RNA level of normal BM2 = 1)

the retrovirus integration site should modify the outcome, so far we did not find any integration that could explain the differing phenotypes of leukemia. Alternatively, it is also possible that types of progenitors transduced with RasGRP4 determine the different phenotypes of leukemia.

Co-transduction of RasGRP4 and AML1-S291fs led to early onset of T cell leukemia as compared with the transduction of RasGRP4 alone. Putting together with clinical reports [2, 9, 36] and our results, we can suggest the significant association of Ras signaling pathway and function of AML1 mutation in leukemogenesis. While AML1 mutations are frequently associated with myeloid leukemia in human patients, they seemed to shorten the latency of T cell leukemia induced by forced expression of RasGRP4 in mouse BMT model. Intriguingly, while RasGRP4 induced c-Kit+/CD3−/CD4+/CD8+ T cell leukemia, combination of RasGRP4 and AML1-S291fs developed more mature T cell leukemia (c-Kit−/CD3+/CD8+/CD4− or CD4+). The reason for this difference is elusive at present. Although we need more cases of BMT mice for confirmation of this difference, AML1-S291fs may also play some roles to induce T cell differentiation in addition to its overall dominant effects on AML1 transcription. In the clinical cases, AML1-LAF4 [37] and AML1-FGA7 [38] were associated with T-ALL, although most of AML1 translocations are associated with myeloid leukemia. Because AML1 is important for transcription of TCR and silencing of CD4, it is possible that AML1-S291fs inhibited the normal ontogeny of T cells, thus accelerating leukemogenic process caused by RasGRP4 in a mice BMT model as a class II mutation that disturbs T cell ontogeny.

Reuther et al. previously isolated RasGRP4 by focus-forming assay of NIH3T3 cells from a patient with AML. This AML-derived RasGRP4 contained a point mutation at codon 620 that changes glutamic acid to lysine at the carboxyl terminus of the protein [29]. However, they found no significant difference in the ability of the AML-derived point mutated RasGRP4 (E620K) or wild-type RasGRP4 (GenBank™ accession number AF448437) in activation of Ras proteins. In our study, we found a gene alteration that induces an amino acid substitution from glutamic acid to lysine at 468 position of RasGRP4 in a patient with MDS/MPD. However, we did not detect a functional difference between RasGRP4 harboring an E468K substitution and RasGRP4 derived from normal volunteers in the ability to abrogate IL-3-dependency of HF6 cells. Moreover, SNPs of this gene are not correlated with lymphoma and leukemia (Y. Nakamura, unpublished results). These results indicate that the sequence difference simply represents a polymorphism or a neutral mutation and has no significant meaning in inducing leukemia. At present, it is not clear whether the sequence alterations in RasGRP4 gene are derived from germ line or somatic mutations.

We found overexpression of RasGRP4 in a patient with T-ALL but it is difficult to conclude the association of RasGRP4 with T-ALL. We also found overexpression of RasGRP4 in some patients with AML-M1, MDS-RAEB, MDS-RA, and CMMoL. The current results suggest that RasGRP4 plays important roles in leukemogenesis in some patients. A clinical study using a large number of patients' samples is required to fully understand the association of RasGRP4 with leukemogenesis.

In summary, we identified RasGRP4 as a candidate gene of class I mutations by our expression cloning strategy based on retrovirus-mediated gene transfer [31, 32, 39]. Although we did not find significant mutations in RasGRP4 derived from patients, overexpression of RasGRP4 confers factor independency on an IL-3 dependent cell line and induced T cell leukemia and myeloid leukemia in a mouse BMT model. Our results indicate possible involvement of RasGRP4 in leukemogenesis.

Acknowledgments We thank Fumi Shibata for technical assistance and Dr. Yusuke Nakamura for the SNPs information of RasGRP4. This work was supported by a grant-in-aid for Cancer Research supported by the Ministry of Health, Labor and Welfare and a grant from the Vehicle Racing Commemorative Foundation.

References

1. Beghini A, Peterlongo P, Ripamonti CB, Larizza L, Cairoli R, Morra E, et al. C-kit mutations in core binding factor leukemias. Blood. 2000;95:726–7.
2. Wang YY, Zhou GB, Yin T, Chen B, Shi JY, Liang WX, et al. AML1-ETO and C-KIT mutation/overexpression in t(8;21) leukemia: implication in stepwise leukemogenesis and response to Gleevec. Proc Natl Acad Sci USA. 2005;102:1104–9. doi: 10.1073/pnas.0408831102.
3. Shimada A, Taki T, Tabuchi K, Tawa A, Horibe K, Tsuchida M, et al. KIT mutations, and not FLT3 internal tandem duplication, are strongly associated with a poor prognosis in pediatric acute myeloid leukemia with t(8;21): a study of the Japanese Childhood AML Cooperative Study Group. Blood. 2006;107:1806–9. doi: 10.1182/blood-2005-08-3408.
4. Yamashita N, Osato M, Huang L, Yanagida M, Kogan SC, Iwasaki M, et al. Haploinsufficiency of Runx1/AML1 promotes myeloid features and leukemogenesis in BXH2 mice. Br J Haematol. 2005;131:495–507. doi:10.1111/j.1365-2141.2005.05793.x.
5. Care RS, Valk PJ, Goodeve AC, Abu-Duhier FM, Geertsma-Kleinekoort WM, Wilson GA, et al. Incidence and prognosis of c-KIT and FLT3 mutations in core binding factor (CBF) acute myeloid leukaemias. Br J Haematol. 2003;121:775–7. doi: 10.1046/j.1365-2141.2003.04362.x.
6. Boissel N, Leroy H, Brethon B, Philippe N, de Botton S, Auvrignon A, et al. Incidence and prognostic impact of c-Kit, FLT3, and Ras gene mutations in core binding factor acute myeloid leukemia (CBF-AML). Leukemia. 2006;20:965–70. doi: 10.1038/sj.leu.2404188.
7. Beghini A, Ripamonti CB, Cairoli R, Cazzaniga G, Colapietro P, Elice F, et al. KIT activating mutations: incidence in adult and pediatric acute myeloid leukemia, and identification of an internal tandem duplication. Haematologica. 2004;89:920–5.
8. Christiansen DH, Andersen MK, Desta F, Pedersen-Bjergaard J. Mutations of genes in the receptor tyrosine kinase (RTK)/RAS-BRAF signal transduction pathway in therapy-related myelodysplasia and acute myeloid leukemia. Leukemia. 2005;19:2232–40. doi:10.1038/sj.leu.2404009.
9. Niimi H, Harada H, Harada Y, Ding Y, Imagawa J, Inaba T, et al. Hyperactivation of the RAS signaling pathway in myelodysplastic syndrome with AML1/RUNX1 point mutations. Leukemia. 2006;20:635–44. doi:10.1038/sj.leu.2404136.
10. Matsuno N, Osato M, Yamashita N, Yanagida M, Nanri T, Fukushima T, et al. Dual mutations in the AML1 and FLT3 genes are associated with leukemogenesis in acute myeloblastic leukemia of the M0 subtype. Leukemia. 2003;17:2492–9. doi: 10.1038/sj.leu.2403160.
11. Roumier C, Eclache V, Imbert M, Davi F, MacIntyre E, Garand R, et al. M0 AML, clinical and biologic features of the disease, including AML1 gene mutations: a report of 59 cases by the Groupe Français d'Hématologie Cellulaire (GFHC) and the Groupe Français de Cytogénétique Hématologique (GFCH). Blood. 2003;101:1277–83. doi:10.1182/blood-2002-05-1474.
12. Callens C, Chevret S, Cayuela JM, Cassinat B, Raffoux E, de Botton S, et al. Prognostic implication of FLT3 and Ras gene mutations in patients with acute promyelocytic leukemia (APL): a retrospective study from the European APL Group. Leukemia. 2005;19:1153–60. doi:10.1038/sj.leu.2403790.
13. Gale RE, Hills R, Pizzey AR, Kottaridis PD, Swirsky D, Gilkes AF, et al. Relationship between FLT3 mutation status, biologic characteristics, and response to targeted therapy in acute promyelocytic leukemia. Blood. 2005;106:3768–76. doi:10.1182/blood-2005-04-1746.
14. Arrigoni P, Beretta C, Silvestri D, Rossi V, Rizzari C, Valsecchi MG, et al. FLT3 internal tandem duplication in childhood acute myeloid leukaemia: association with hyperleucocytosis in acute promyelocytic leukaemia. Br J Haematol. 2003;120:89–92. doi: 10.1046/j.1365-2141.2003.04032.x.
15. Noguera NI, Breccia M, Divona M, Diverio D, Costa V, De Santis S, et al. Alterations of the FLT3 gene in acute

promyelocytic leukemia: association with diagnostic characteristics and analysis of clinical outcome in patients treated with the Italian AIDA protocol. Leukemia. 2002;16:2185–9. doi:10.1038/sj.leu.2402723.
16. Kainz B, Heintel D, Marculescu R, Schwarzinger I, Sperr W, Le T, et al. Variable prognostic value of FLT3 internal tandem duplications in patients with de novo AML and a normal karyotype, t(15;17), t(8;21) or inv(16). Hematol J. 2002;3:283–9. doi:10.1038/sj.thj.6200196.
17. Taketani T, Taki T, Sugita K, Furuichi Y, Ishii E, Hanada R, et al. FLT3 mutations in the activation loop of tyrosine kinase domain are frequently found in infant ALL with MLL rearrangements and pediatric ALL with hyperdiploidy. Blood. 2004;103:1085–8. doi:10.1182/blood-2003-02-0418.
18. Liang DC, Shih LY, Fu JF, Li HY, Wang HI, Hung IJ, et al. K-Ras mutations and N-Ras mutations in childhood acute leukemias with or without mixed-lineage leukemia gene rearrangements. Cancer. 2006;106:950–6. doi:10.1002/cncr.21687.
19. Gale RE, Green C, Allen C, Mead AJ, Burnett AK, Hills RK, et al. The impact of FLT3 internal tandem duplication mutant level, number, size, and interaction with NPM1 mutations in a large cohort of young adult patients with acute myeloid leukemia. Blood. 2008;111:2776–84. doi:10.1182/blood-2007-08-109090.
20. Kiyoi H, Naoe T, Nakano Y, Yokota S, Minami S, Miyawaki S, et al. Prognostic implication of FLT3 and N-RAS gene mutations in acute myeloid leukemia. Blood. 1999;93:3074–80.
21. Stirewalt DL, Kopecky KJ, Meshinchi S, Appelbaum FR, Slovak ML, Willman CL, et al. FLT3, RAS, and TP53 mutations in elderly patients with acute myeloid leukemia. Blood. 2001;97:3589–95. doi:10.1182/blood.V97.11.3589.
22. Kelly LM, Kutok JL, Williams IR, Boulton CL, Amaral SM, Curley DP, et al. PML/RARalpha and FLT3-ITD induce an APL-like disease in a mouse model. Proc Natl Acad Sci USA. 2002;99:8283–8. doi:10.1073/pnas.122233699.
23. Warner JK, Wang JC, Takenaka K, Doulatov S, McKenzie JL, Harrington L, et al. Direct evidence for cooperating genetic events in the leukemic transformation of normal human hematopoietic cells. Leukemia. 2005;19:1794–805. doi:10.1038/sj.leu.2403917.
24. Gilliland DG, Griffin JD. Role of FLT3 in leukemia. Curr Opin Hematol. 2002;9:274–81. doi:10.1097/00062752-200207000-00003.
25. Schessl C, Rawat VP, Cusan M, Deshpande A, Kohl TM, Rosten PM, et al. The AML1-ETO fusion gene and the FLT3 length mutation collaborate in inducing acute leukemia in mice. J Clin Invest. 2005;115:2159–68. doi:10.1172/JCI24225.
26. Cuenco GM, Ren R. Cooperation of BCR-ABL and AML1/MDS1/EVI1 in blocking myeloid differentiation and rapid induction of an acute myelogenous leukemia. Oncogene. 2001;20:8236–48. doi:10.1038/sj.onc.1205095.
27. Ono R, Nakajima H, Ozaki K, Kumagai H, Kawashima T, Taki T, et al. Dimerization of MLL fusion proteins and FLT3 activation synergize to induce multiple-lineage leukemogenesis. J Clin Invest. 2005;115:919–29.
28. Chan IT, Kutok JL, Williams IR, Cohen S, Moore S, Shigematsu H, et al. Oncogenic K-ras cooperates with PML-RAR alpha to induce an acute promyelocytic leukemia-like disease. Blood. 2006;108:1708–15. doi:10.1182/blood-2006-04-015040.
29. Reuther GW, Lambert QT, Rebhun JF, Caligiuri MA, Quilliam LA, Der CJ. RasGRP4 is a novel Ras activator isolated from acute myeloid leukemia. J Biol Chem. 2002;277:30508–14. doi:10.1074/jbc.M111330200.
30. Yang Y, Li L, Wong GW, Krilis SA, Madhusudhan MS, Sali A, et al. RasGRP4, a new mast cell-restricted Ras guanine nucleotide-releasing protein with calcium- and diacylglycerol-binding motifs Identification of defective variants of this signaling protein in asthma, mastocytosis, and mast cell leukemia patients and demonstration of the importance of RasGRP4 in mast cell development and function. J Biol Chem. 2002;277:25756–74. doi:10.1074/jbc.M202575200.
31. Kitamura T, Onishi M, Kinoshita S, Shibuya A, Miyajima A, Nolan GP. Efficient screening of retroviral cDNA expression libraries. Proc Natl Acad Sci USA. 1995;92:9146–50. doi:10.1073/pnas.92.20.9146.
32. Kitamura T, Koshino Y, Shibata F, Oki T, Nakajima H, Nosaka T, et al. Retrovirus-mediated gene transfer and expression cloning: powerful tools in functional genomics. Exp Hematol. 2003;31:1007–14.
33. Harada H, Harada Y, Niimi H, Kyo T, Kimura A, Inaba T. High incidence of somatic mutations in the AML1/RUNX1 gene in myelodysplastic syndrome and low blast percentage myeloid leukemia with myelodysplasia. Blood. 2004;103:2316–24. doi:10.1182/blood-2003-09-3074.
34. Izawa K, Kitaura J, Yamanishi Y, Matsuoka T, Oki T, Shibata F, et al. Functional analysis of activating receptor LMIR4 as a counterpart of inhibitory receptor LMIR3. J Biol Chem. 2007;282:17997–8008. doi:10.1074/jbc.M701100200.
35. Watanabe-Okochi N, Kitaura J, Ono R, Harada H, Harada Y, Komeno Y, et al. AML1 mutations induced MDS and MDS/AML in a mouse BMT model. Blood. 2008;111:4297–308. doi:10.1182/blood-2007-01-068346.
36. Reuss-Borst MA, Bühring HJ, Schmidt H, Müller CA. AML: immunophenotypic heterogeneity and prognostic significance of c-kit expression. Leukemia. 1994;8:258–63.
37. Chinen Y, Taki T, Nishida K, Shimizu D, Okuda T, Yoshida N, et al. Identification of the novel AML1 fusion partner gene, LAF4, a fusion partner of MLL, in childhood T cell acute lymphoblastic leukemia with t(2;21)(q11;q22) by bubble PCR method for cDNA. Oncogene. 2008;27:2249–56. doi:10.1038/sj.onc.1210857.
38. Mikhail FM, Coignet L, Hatem N, Mourad ZI, Farawela HM, El Kaffash DM, et al. A novel gene, FGA7, is fused to RUNX1/AML1 in a t(4;21)(q28;q22) in a patient with T cell acute lymphoblastic leukemia. Genes Chromosomes Cancer. 2004;39:110–8. doi:10.1002/gcc.10302.
39. Kitamura T. New experimental approaches in retrovirus-mediated expression screening. Int J Hematolv. 1998;67:351–9. doi:10.1016/S0925-5710(98)00025-5.

The Journal of Immunology

An Activating and Inhibitory Signal from an Inhibitory Receptor LMIR3/CLM-1: LMIR3 Augments Lipopolysaccharide Response through Association with FcR{gamma} in Mast Cells

Kumi Izawa, Jiro Kitaura, Yoshinori Yamanishi, Takayuki Matsuoka, Ayako Kaitani, Masahiro Sugiuchi, Mariko Takahashi, Akie Maehara, Yutaka Enomoto, Toshihiko Oki, Toshiyuki Takai and Toshio Kitamura

J. Immunol. 2009;183;925-936; originally published online Jun 26, 2009;
doi:10.4049/jimmunol.0900552
http://www.jimmunol.org/cgi/content/full/183/2/925

The Journal of Immunology is published twice each month by The American Association of Immunologists, Inc., 9650 Rockville Pike, Bethesda, MD 20814-3994.

Print ISSN: 0022-1767 Online ISSN: 1550-6606.

An Activating and Inhibitory Signal from an Inhibitory Receptor LMIR3/CLM-1: LMIR3 Augments Lipopolysaccharide Response through Association with FcRγ in Mast Cells[1]

Kumi Izawa,* Jiro Kitaura,* Yoshinori Yamanishi,* Takayuki Matsuoka,* Ayako Kaitani,* Masahiro Sugiuchi,* Mariko Takahashi,* Akie Maehara,* Yutaka Enomoto,* Toshihiko Oki,* Toshiyuki Takai,† and Toshio Kitamura[2]*

Leukocyte mono-Ig-like receptor 3 (LMIR3) is an inhibitory receptor mainly expressed in myeloid cells. Coengagement of FcεRI and LMIR3 impaired cytokine production in bone marrow-derived mast cells (BMMCs) induced by FcεRI crosslinking alone. Mouse LMIR3 possesses five cytoplasmic tyrosine residues (Y241, Y276, Y289, Y303, Y325), among which Y241 and Y289 (Y241/289) or Y325 fit the consensus sequence of ITIM or immunotyrosine-based switch motif (ITSM), respectively. The inhibitory effect was abolished by the replacement of Y325 in addition to Y241/289 with phenylalanine (Y241/189/325/F) in accordance with the potential of Y241/289/325 to cooperatively recruit Src homology region 2 domain-containing phosphatase 1 (SHP)-1 or SHP-2. Intriguingly, LMIR3 crosslinking alone induced cytokine production in BMMCs expressing LMIR3 (Y241/276/289/303/325F) mutant as well as LMIR3 (Y241/289/325F). Moreover, coimmunoprecipitation experiments revealed that LMIR3 associated with ITAM-containing FcRγ. Analysis of FcRγ-deficient BMMCs demonstrated that both Y276/303 and FcRγ played a critical role in the activating function of this inhibitory receptor. Importantly, LMIR3 crosslinking enhanced cytokine production of BMMCs stimulated by LPS, while suppressing production stimulated by other TLR agonists or stem cell factor. Thus, an inhibitory receptor LMIR3 has a unique property to associate with FcRγ and thereby functions as an activating receptor in concert with TLR4 stimulation. ***The Journal of Immunology,*** **2009, 183: 925–936.**

The immune system is tightly regulated by the balance of activating and inhibitory signals through a variety of immune receptors. Paired immune receptors are generally composed of several activating and inhibitory receptors with high homology in the extracellular domains (1, 2). We have previously characterized leukocyte mono-Ig-like receptors 1–5 (LMIR1–5)[3] among a novel paired receptor family called LMIR/CMRF-35-like molecules (CLMs)/myeloid-associated Ig-like receptor (MAIR)/dendritic cell-derived Ig-like receptor (DIgR)/CD300 (3–9). LMIR3/CLM-1/MAIR-V/DIgR2/CD300LF is an inhibitory receptor that possesses an ITIM in the cytoplasmic region (4, 6, 7, 10, 11). On the other hand, LMIR4/CLM-5 or LMIR5/CLM-7, which is an activating receptor paired with LMIR3, associates with an ITAM-containing adaptor protein, FcRγ or DNAX activating protein of 12 kDa (DAP12), respectively (4, 11, 12). LMIR3 is mainly expressed in myeloid cells such as granulocytes, dendritic cells, and mast cells. Recent studies have demonstrated that LMIR3 is an inhibitory receptor that can block osteoclastogenesis (6), negatively regulate dendritic cell-initiated Ag-specific T cell responses (11), or impair cytokine production in mast cells (4, 6). The finding that intraperitoneal administration of LPS or G-CSF up-regulates LMIR3 in granulocytes implicates LMIR3 in innate immunity or cell differentiation (4).

Mast cells are important effector cells not only in IgE-associated allergic disorders but also in innate immunity (13–15). Several inhibitory receptors belonging to paired immune receptors are expressed in mast cells: FcγRIIB (16), gp49B1 (17), paired Ig-like receptor-B (PIR-B) (18, 19), and LMIR1/CD300A (3, 20, 21). These receptors inhibit FcεRI-mediated activating signal transduction, but how they regulate innate immune response in mast cells remains obscure.

Structurally, mouse LMIR3 contains five cytoplasmic tyrosine residues (Y241, Y276, Y289, Y303, or Y325), among which both Y241 and Y289 are located in ITIM (S/I/V/LxYxxI/V/L) and Y325 is located in the immunoreceptor tyrosine-based switch motif (ITSM) (TxYxxV/I) (22). Like ITIM, ITSM can associate with the SH2-containing tyrosine phosphatases Src homology region 2 domain-containing phosphatase 1 (SHP)-1 and SHP-2 or the SH2-containing inositol phosphatase SHIP (22, 23). On the other hand,

*Division of Cellular Therapy, Advanced Clinical Research Center, The Institute of Medical Science, The University of Tokyo, Tokyo, Japan; and the †Department of Experimental Immunology, Institute of Development, Aging and Cancer, Tohoku University, Sendai, Japan

Received for publication February 20, 2009. Accepted for publication May 18, 2009.

The costs of publication of this article were defrayed in part by the payment of page charges. This article must therefore be hereby marked *advertisement* in accordance with 18 U.S.C. Section 1734 solely to indicate this fact.

[1] This work was supported by the Ministry of Education, Science, Technology, Sports and Culture and the Ministry of Health and Welfare, Japan.

[2] Address correspondence and reprint requests to Dr. Toshio Kitamura, Division of Cellular Therapy, Advanced Clinical Research Center, The Institute of Medical Science, The University of Tokyo, 4-6-1 Shirokanedai, Minato-ku, Tokyo 108-8639, Japan. E-mail address: kitamura@ims.u-tokyo.ac.jp

[3] Abbreviations used in this paper: LMIR, leukocyte mono-Ig-like receptor; BMMC, bone marrow-derived mast cell; CLM, CMRF-35-like molecule; DAP10, DNAX activating protein of 10 kDa; IREM-1, immune receptor expressed on myeloid cells 1; ITSM, immunotyrosine-based switch motif; ODN, oligodeoxynucleotide; SHP, Src homology region 2 domain-containing phosphatase 1; SCF, stem cell factor; TNP, trinitrophenyl; WT, wild type.

www.jimmunol.org/cgi/doi/10.4049/jimmunol.0900552

unlike ITIM, ITSM binds to adaptor molecules, such as SH2-containing adaptor protein SH2 domain protein 1A (SH2D1A) and EWS-activated transcript 2 (EAT-2), as well as to Src family kinases and the p85 regulatory subunit of PI3K (22–23). Whether an ITSM transduces an activating or an inhibitory signal depends on the immune receptor and cell type. Additionally, Y276 or Y303 of LMIR3 is situated in the putative binding motif for p85 (YxxM) or Grb2 (YxN), respectively. The existence of these signaling motifs in the cytoplasmic region of LMIR3 indicates the potential of an inhibitory LMIR3 to function as an activating receptor. In fact, as recently reported by Alvarez-Errico et al., immune receptor expressed on myeloid cells 1 (IREM-1), a human homolog of mouse LMIR3, transmitted a PI3K-dependent activating signal in rat basophil leukemia (RBL) cells transduced with an IREM-1 mutant that lost inhibitory function by the replacement of several tyrosine residues with phenylalanine (24, 25). However, the biological significance of the activating function of endogenous LMIR3 remains unknown.

In the present study, we demonstrate the dual functions, inhibitory and activating, of mouse LMIR3 in mast cells. Examination of the contribution of each cytoplasmic tyrosine residue to the dual functions revealed that ITSM in addition to ITIM was required for the inhibitory function, while Y276 and Y303 were involved in the activating function. Surprisingly, LMIR3 mediated an activating signal mainly through its association with FcRγ; it is unprecedented that an ITIM-bearing receptor functions as an activating receptor by associating with an ITAM-bearing adaptor. Importantly, we delineated the biological situation where LMIR3 mediated either an inhibitory or an activating function. Notably, this positive signal of LMIR3 synergizes with TLR4 stimulation.

Materials and Methods

Abs and reagents

Rat anti-LMIR3 IgG2a mAb, designated anti-LMIR3 mAb, and goat anti-LMIR3 polyclonal Ab were obtained from R&D Systems. Anti-FLAG mAb M2, FITC-conjugated anti-FLAG mAb M2, rabbit anti-FLAG polyclonal Ab, mouse IgG1 mAb (MOPC21), and mouse anti-DNP IgE mAb (clone SPE-7; designated SPE-7 IgE) were all purchased from Sigma-Aldrich. Mouse anti-Myc mAb (9E10) was from Roche Diagnostics. Mouse anti-trinitrophenyl (TNP) IgE mAb (C38-2) and FITC-conjugated anti-mouse IgE mAb were from BD Biosciences. PE-conjugated anti-c-Kit mAb and rat IgG2a were from eBioscience. Anti-ERK, anti-Akt, anti-SH-PTP1 (C-19), anti-SH-PTP2 (C-18), anti-SHIP (N-1), and anti-Grb2 (C-23) Abs were from Santa Cruz Biotechnology. Mouse anti-phosphotyrosine mAb (4G10), rabbit anti-phosphotyrosine polyclonal Ab, rabbit anti-FcεRI-γ subunit polyclonal Ab, and rabbit anti-PI3K p85 polyclonal Ab were purchased from Upstate Biotechnology. All other phospho-specific Abs were purchased from Cell Signaling Technology. Rabbit $F(ab')_2$ anti-rat IgG(H+L) was from SouthernBiotech. Goat anti-mouse IgG(H+L) was from Zymed Laboratories. $F(ab')_2$ fragments were prepared by digesting anti-FLAG mAb M2 or mouse IgG1 mAb with immobilized pepsin, followed by removing intact mAb by protein A affinity chromatography (Pierce). Cytokines were obtained from R&D Systems. Zymosan, poly(I:C), and oligodeoxynucleotide (ODN)1585 were purchased from InvivoGen. All other reagents were from Sigma-Aldrich unless stated otherwise.

Cell culture and isolation

Ba/F3 cells and COS-7 cells were cultured as described (4). CBA/J or C57BL/6 mice (Charles River Laboratories) were used at 8–10 wk of age for isolation of cells. To generate bone marrow-derived mast cells (BMMCs) with 90% purity (c-kit$^+$/FcεRI$^+$ by flow cytometry), BMMCs were cultured in the presence of 10 ng/ml IL-3 alone or with 20 ng/ml stem cell factor (SCF), respectively, as described (4, 5, 26). The following mutant mice were used: *FcRγ*$^{-/-}$ (27).

Stimulation

In the coligation of FcεRI and endogenous LMIR3, MaxiSorp 96-well plates (Nunc, catalog no. 430341) were overnight incubated with $F(ab')_2$ anti-rat IgG Ab (SouthernBiotec), which recognized mouse IgE as well as anti-LMIR3 Ab (rat IgG2a). After BMMCs were sensitized with 0.5 μg/ml anti-TNP IgE overnight and washed twice, they were preincubated with 20 μg/ml anti-LMIR3 Ab or rat IgG2a for 1 h on ice and washed twice before stimulation with plate-coated secondary Ab. In the coligation of FcεRI and FLAG-tagged LMIR3 or LMIR1 in the transduced BMMCs, after sensitization with 0.5 μg/ml anti-TNP IgE overnight, they were preincubated with 20 μg/ml $F(ab')_2$ anti-FLAG or mouse IgG1 mAb for 1 h on ice and washed twice before stimulation with plate-coated $F(ab')_2$ anti-mouse IgG Ab (Zymed Laboratories), which recognized mouse IgE as well as $F(ab')_2$ anti-FLAG mAb (mouse IgG1). In the case of LMIR3 or LMIR1 crosslinking with or without other stimuli, LMIR was engaged by using plate-coated Ab as described in the presence or not of 10 or 100 ng/ml LPS, 100 μg/ml zymosan, 250 μg/ml poly(I:C), 5 μg/ml ODN1585, and100 ng/ml SCF. Alternatively, BMMCs were directly stimulated with 5 μg/ml SPE-7 IgE or 100 nM PMA. In the coimmunoprecipitation experiments using Ba/F3 cells, Ba/F3 cells were stimulated by 100 μM sodium pervanadate for 10 min.

Plasmid constructs

An expression plasmid encoding Myc epitope-tagged DNAX activating protein of 10 kDa (DAP10), DAP12, or FcRγ was generated as described (3–5). Signaling lymphocyte activation molecule (SLAM) signal sequence (provided by Dr. H. Arase, Osaka University) (28) Myc-DAP10, DAP12, or FcRγ fragment was subcloned into pMXs-IRES-blasticidin (pMXs-IB) (29), generating pMXs-Myc-DAP10, DAP12, or FcRγ-IB. The entire sequences excluding the leader sequence of LMIR3 and LMIR1 were amplified, and the resulting fragment was ligated into a pME vector including the signal sequence of SLAM. The resulting SLAM signal sequence-FLAG-LMIR3 or LMIR1 fragment was subcloned into pMXs-IRES-puro (pMXs-IP) generating pMXs-FLAG-LMIR3 or LMIR1-IP (29). To generate different LMIR3 mutants where one or several tyrosine residues among five cytoplasmic tyrosine residues (Y241, Y276, Y289, Y303, or Y325) are replaced with phenylalanine, two-step PCR mutagenesis was performed by using pMXs-FLAG-LMIR3 or LMIR3 mutant-IP as a template. To generate LMIR1 mutant where both Y258 and Y270 in the cytoplasmic region were replaced phenylalanine, two-step PCR mutagenesis was also performed by using pMXs-FLAG-LMIR1-IP as a template. All constructs were verified by DNA sequencing.

Transfection and infection

Retroviral transfection was as described (3–5). Briefly, retroviruses were generated by transient transfection of Plat-E packaging cells (29) with FuGENE 6 (Roche Diagnostics). Cells were infected with retroviruses in the presence of 10 μg/ml polybrene. Selection with puromycin was started 48 h after infection (30).

Biochemistry

To detect the association of LMIR3 and FcRγ, COS-7 cells were cotransfected with two constructs of interest (pMXs-FLAG-LMIR3-IP and pMXs-Myc-DAP10, DAP12, or FcRγ-IB) or (pMXs-FLAG-LMIR3 (WT), LMIR3 (Y1/3/5F), or LMIR3 (YallF)-IP and pMXs-Myc-FcRγ-IB). Cell lysis, immunoprecipitation, and Western blotting were as described (3–5).

Flow cytometry

Flow cytometric analysis of the stained cells was performed with a FACSCalibur (BD Biosciences) equipped with CellQuest software and FlowJo software (Tree Star) as described (3–5).

Measurement of cytokines

Culture supernatants of stimulated BMMCs were measured using ELISA kits of IL-6 or TNF-α from R&D Systems as described (3–5).

Statistical analysis

Data are shown as the means ± SD, and statistical significance was determined by Student's *t* test, with $p < 0.05$ taken as statistically significant.

Results

The inhibitory effect of LMIR3 on FcεRI-mediated cytokine production in mast cells

We generated BMMCs with 95% purity (FcεRI$^+$/c-kit$^+$) and confirmed surface expression of endogenous LMIR3 in BMMCs by using anti-LMIR3 Ab (Fig. 1*A*). IgE-bound FcεRI in BMMCs was engaged by plate-coated $F(ab')_2$ anti-rat IgG Ab (see *Materials*

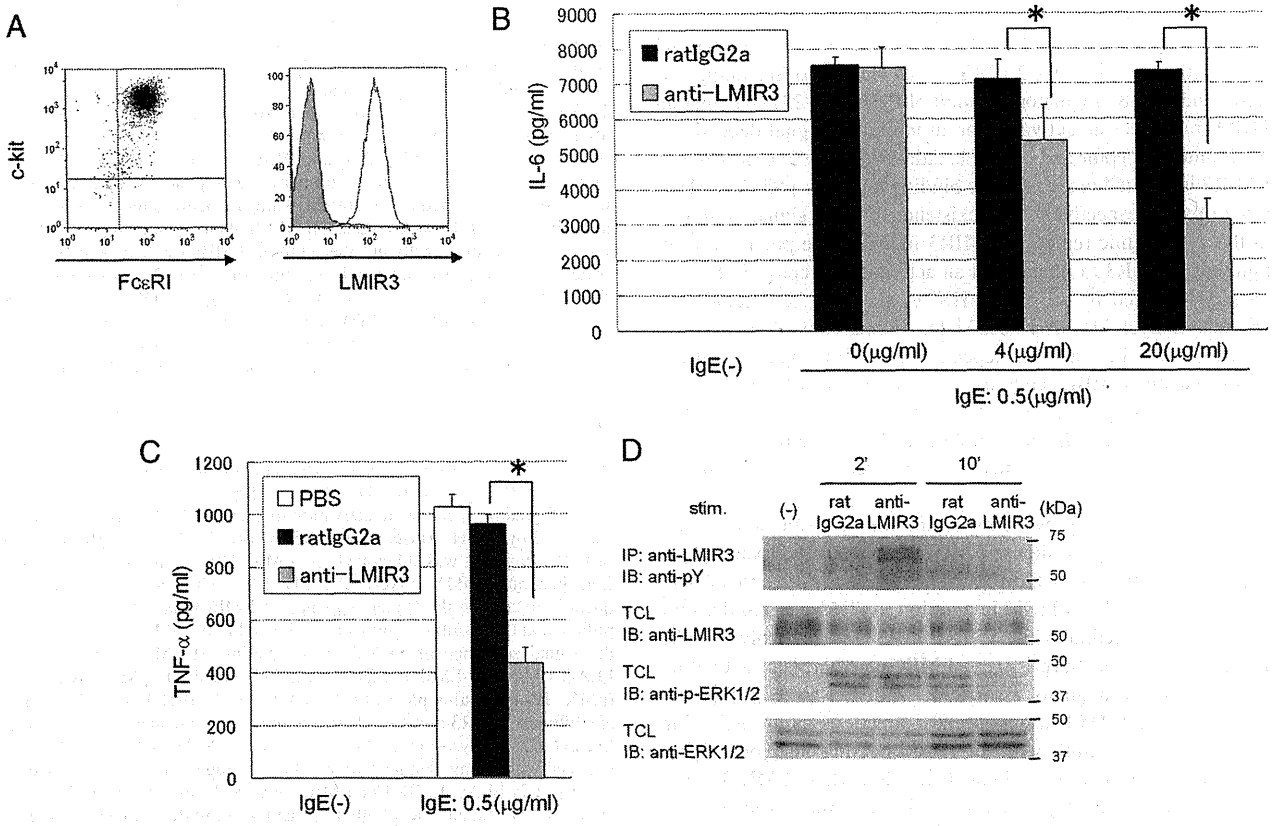

FIGURE 1. Coligation of FcεRI and LMIR3 in BMMCs impaired cytokine production induced by FcεRI crosslinking alone. *A*, Surface expression levels of c-kit and IgE-bound FcεRI (*left panel*) as well as those of endogenous LMIR3 (*right panel*) in BMMCs were analyzed by flow cytometry. *B*, IgE-bound or unbound FcεRI and endogenous LMIR3 in BMMCs were coligated by various concentrations (0, 4, 20 μg/ml) of anti-LMIR3 Ab or rat IgG2a Ab as control on $F(ab')_2$ anti-rat IgG Ab-coated plates as described in *Materials and Methods*. IL-6 released into the culture supernatants was measured by ELISA. All data points correspond to the mean and the SD of three independent experiments. Rat IgG2a or anti-LMIR3 indicates rat IgG2a Ab or rat anti-LMIR3 Ab, respectively. IgE(+) or IgE(−) indicates BMMCs sensitized with IgE or not, respectively. *C*, IgE-bound FcεRI and endogenous LMIR3 in BMMCs were coligated in BMMCs using 20 μg/ml anti-LMIR3 Ab, rat IgG2a Ab, or PBS on $F(ab')_2$ anti-rat IgG Ab-coated plates. TNF-α released into the culture supernatants was measured by ELISA. All data points correspond to the mean and the SD of three independent experiments. *D*, IgE-bound FcεRI and endogenous LMIR3 in BMMCs were coligated in BMMCs using 20 μg/ml anti-LMIR3 Ab or 20 μg/ml rat IgG2a Ab as control on $F(ab')_2$ anti-rat IgG Ab-coated plates for 2 or 10 min. Cell lysates were subjected to immunoblotting with anti-phospho-p44/42 MAPK (pERK1/2) Ab. Equal loading was evaluated by reprobing the immunoblots with anti-ERK1/2 Ab or anti-LMIR3 Ab. Immunoprecipitates of cell lysates with anti-LMIR3 Ab were immunoblotted with anti-phosphotyrosine (pY) mAb. *, $p < 0.05$.

and Methods), resulting in cytokine production of BMMCs in an IgE-dose dependent manner (supplemental Fig. S1*A*).[4] Since LMIR3 contains ITIM in the cytoplasmic region, the role of LMIR3 as an inhibitory receptor was expected in mast cells. Indeed, coligation of anti-LMIR3 Ab-bound LMIR3 and IgE-bound FcεRI in BMMCs significantly impaired the cytokine (IL-6 and TNF-α) production induced by crosslinking of IgE-bound FcεRI alone (see *Materials and Methods* and Fig. 1, *B* and *C*). No detectable cytokine production was observed in BMMCs stimulated by LMIR3 crosslinking alone (Fig. 1, *B* and *C*). Additionally, anti-LMIR3 Ab, but not control Ab, dose-dependently suppressed IL-6 production, suggesting an LMIR3-dependent inhibitory effect on FcεRI-mediated cytokine production in mast cells (Fig. 1*B*). Furthermore, Western blot analysis demonstrated increased tyrosine phosphorylation of LMIR3 at 2 min followed by attenuated ERK phosphorylation at 10 min after the coligation (Fig. 1*D*), indicating the involvement of LMIR3 cytoplasmic tyrosine residues in the inhibitory signal.

[4] The online version of this article contains supplemental material.

Y325 in addition to Y241 and Y289 played an important role in the inhibitory function of LMIR3 in mast cells

LMIR3 contains five cytoplasmic tyrosine residues, Y241, Y276, Y289, Y303, and Y325, which are hereafter abbreviated as Y1, Y2, Y3, Y4, and Y5, respectively (Fig. 2*D*). To investigate the role in the inhibitory function of each cytoplasmic tyrosine residue, we generated FLAG-tagged wild-type (WT) LMIR3 and different mutants where one or several cytoplasmic tyrosine residues were replaced with phenylalanine, as depicted in Fig. 2*D* and Table I. First, BMMCs with 95% purity ($Fc\varepsilon RI^+$/$c\text{-}kit^+$) were retrovirally transduced with FLAG-tagged LMIR3(WT) (Fig. 2*A*, *left panel*). Surface expression of transduced LMIR3 in BMMCs was confirmed by using anti-FLAG Ab (Fig. 2*A*, *right panel*). We also confirmed that IgE-bound FcεRI in BMMCs was engaged by plate-coated $F(ab')_2$ anti-mouse IgG Ab (see *Materials and Methods*), leading to cytokine production of BMMCs in an IgE-dose dependent manner (supplemental Fig. S1*B*). As with endogenous LMIR3, transduced FLAG-tagged LMIR3(WT) displayed an inhibitory effect on FcεRI-mediated IL-6 production and ERK activation of BMMCs (see *Materials and Methods* and Fig. 2, *B* and

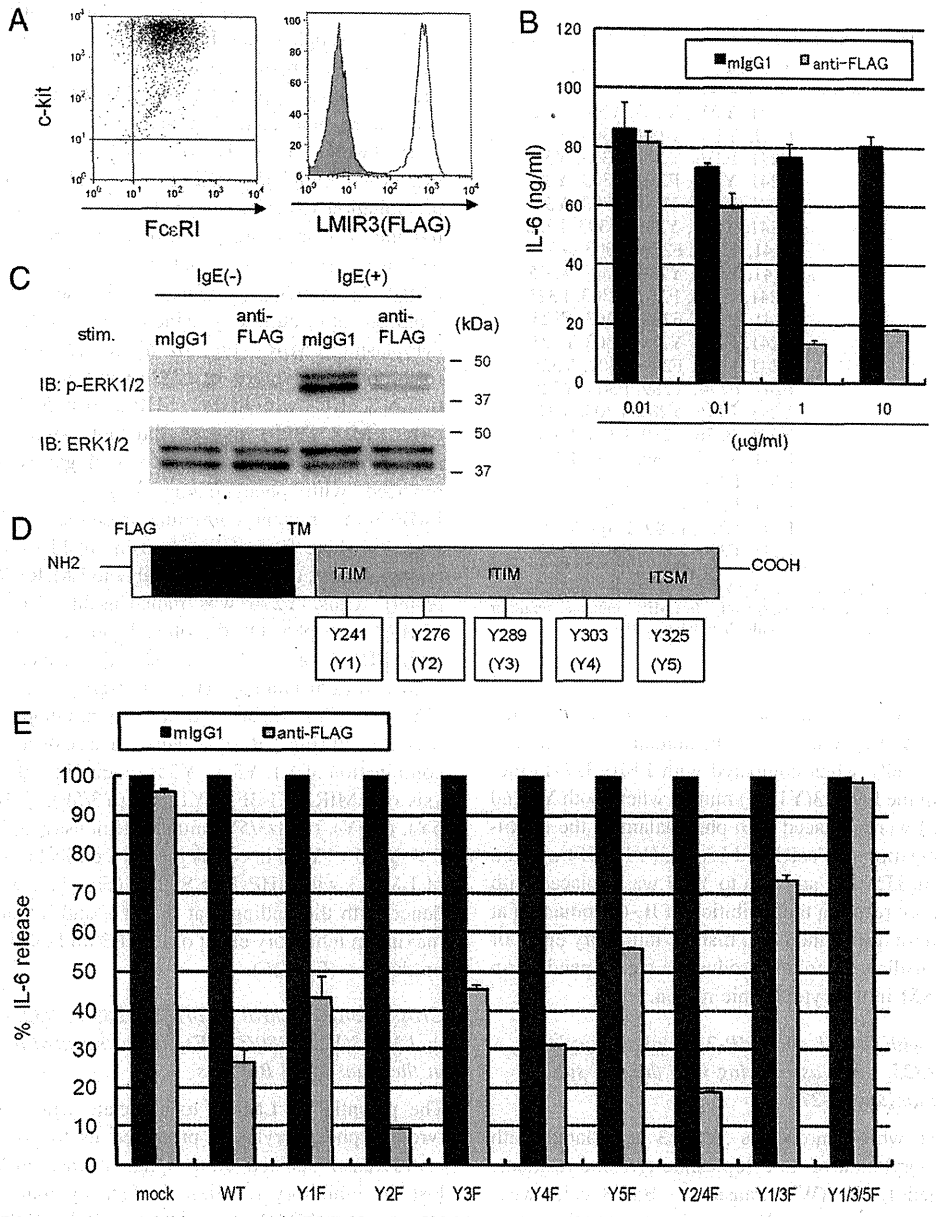

FIGURE 2. LMIR3 transmits an inhibitory signal in BMMCs via Y325 located in ITSM in addition to Y241/Y289 located in ITIM. *A*, BMMCs from mice were transduced with FLAG-tagged LMIR3. Surface expression levels of c-kit and IgE-bound FcεRI as well as those of FLAG-tagged LMIR3 were analyzed by flow cytometry. *B*, IgE-bound FcεRI and FLAG-tagged LMIR3 in the transduced BMMCs were coligated by using various concentrations (0, 0.1, 1, 10 μg/ml) of $F(ab')_2$ anti-FLAG mAb or mouse IgG1 mAb as control on $F(ab')_2$ anti-mouse IgG Ab-coated plates as described in *Materials and Methods*. IL-6 released into the culture supernatants was measured by ELISA. All data points correspond to the mean and the SD of three independent experiments. mIgG1 or anti-FLAG indicates $F(ab')_2$ mouse IgG1 mAb or $F(ab')_2$ anti-FLAG mAb. *C*, IgE-bound or unbound FcεRI and FLAG-tagged LMIR3 in the transduced BMMCs were coligated by 10 μg/ml $F(ab')_2$ anti-FLAG mAb or 10 μg/ml mouse IgG1 mAb as control on $F(ab')_2$ anti-mouse IgG Ab-coated plates for 10 min. Cell lysates were subject to immunoblotting with anti-phospho-p44/42 MAPK (pERK1/2) Ab. Equal loading was evaluated by reprobing the immunoblot with anti-ERK1/2 Ab. IgE(+) or IgE(−) indicates BMMCs sensitized with IgE or not, respectively. *D*, Structure of FLAG-tagged LMIR3(WT) containing cytoplasmic five tyrosine residues, Y241, Y276, Y289, Y303, and Y325, abbreviated as Y1, Y2, Y3, Y4, and Y5, respectively. Y1 and Y3 are located in ITIM, while Y5 is located in ITSM. TM indicates the transmembrane region. *E*, The ratio of the amounts of IL-6 produced by each transfectant when FLAG-tagged LMIR3 mutant and IgE-bound FcεRI were coligated by using $F(ab')_2$ anti-FLAG mAb to those only when IgE-bound FcεRI was engaged by using $F(ab')_2$ mouse IgG1 mAb. BMMCs were transduced with FLAG-tagged LMIR3(WT), different mutants, or mock. Data are representative of three independent experiments. All data points correspond to the mean and the SD.

C). Next, we generated different LMIR3 mutant-transduced BMMCs that showed equivalent levels of mast cell maturity and surface LMIR3 expression, although higher expression levels of LMIR3 were observed in LMIR3(YallF) mutant-transduced BMMCs (supplemental Fig. S2). To examine the inhibitory effect of each LMIR3 mutant, we measured the ratio of the amounts of IL-6 produced by each transfectant when FLAG-tagged LMIR3 mutants and FcεRI were coligated to those when FcεRI was engaged alone, as described in *Materials and Methods*. As demonstrated in Fig. 2*E*, LMIR3(WT)-mediated inhibition of IL-6 production was ~75%. Among LMIR3 mutants, LMIR3(Y2F), (Y4F), or (Y2/4F) mutant-mediated inhibition was 70–90%, indicating that Y2 and